1521-0111/85/1/50–61$25.00
MOLECULAR PHARMACOLOGY

http://dx.doi.org/10.1124/mol.113.088484
Mol Pharmacol 85:50–61, January 2014

The α4 Nicotinic Receptor Promotes CD4$^+$ T-Cell Proliferation and a Helper T-Cell Immune Response[S]

Jacob C. Nordman, Pretal Muldoon, Sarah Clark, M. Imad Damaj, and Nadine Kabbani

Department of Molecular Neuroscience, Krasnow Institute for Advanced Study, George Mason University, Fairfax, Virginia (J.C.N., S.C., N.K.); and Department of Pharmacology and Toxicology, Virginia Commonwealth University, Richmond, Virginia (P.M., M.I.D.)

Received July 15, 2013; accepted October 9, 2013

ABSTRACT

Smoking is a common addiction and a leading cause of disease. Chronic nicotine exposure is known to activate nicotinic acetylcholine receptors (nAChRs) in immune cells. We demonstrate a novel role for α4 nAChRs in the effect of nicotine on T-cell proliferation and immunity. Using cell-based sorting and proteomic analysis we define an α4 nAChR expressing helper T-cell population (α4$^+$CD3$^+$CD4$^+$) and show that this group of cells is responsive to sustained nicotine exposure. In the circulation, spleen, bone marrow, and thymus, we find that nicotine promotes an increase in CD3$^+$CD4$^+$ cells via its activation of the α4 nAChR and regulation of G protein subunit o, G protein regulated–inducer of neurite outgrowth, and CDC42 signaling within T cells. In particular, nicotine is found to promote a helper T cell 2 adaptive immunologic response within T cells that is absent in α4$^{-/-}$ mice. We thus present a new mechanism of α4 nAChR signaling and immune regulation in T cells, possibly accounting for the effect of smoking on the immune system.

Introduction

Smoking is one of the most prevalent addictions and comes replete with numerous health risks. Among these, smoking has been implicated as a causative agent for various disorders including most cancers, cardiovascular disease, and autoimmune diseases such as lupus and myasthenia gravis (Moreau et al., 1994; Costenbader and Karlson, 2005). Nicotine appears to target lymphatic organs such as the spleen, thymus, and lymph nodes and has been shown to play a role in bacterial immunity (Andersson, 2005), increased interleukin-6 (IL-6) production in the spleen (Song et al., 1999), and T-cell maturation (Middlebrook et al., 2002). Recent studies show a connection between cigarette smoke and the helper T-cell (T_H) driven T_H1/T_H2 division of immunity, in which smoking promotes T_H2-related adaptive immunologic responses (Zhang and Petro, 1996).

The molecular target of nicotine is a class of ligand-gated ion channels also activated by the endogenous neurotransmitter acetylcholine (Changeux, 2010). In mammals, 17 subunits (α1–α7, α9, α10, β1–β4, γ, δ, and ε) confer the expression of a functional nicotinic acetylcholine receptor (nAChR) in cells (Changeux, 2010). A subset of nAChRs have been discovered in immune cells (Kawashima and Fujii, 2003), but to date a nicotinic-activated current has not been detected in lymphocytes. Clearly, however, a number of systems, including the neural immune "inflammatory reflex," depend on the activity of nAChRs. For example, cytokine-producing macrophages in the spleen contain α7 nAChRs, which regulate the activity of the vagus nerve (Rosas-Ballina et al., 2011). The α7 nAChR agonists, including nicotine, appear to regulate cytokine production in immune cells of the lung and spleen, suggesting that nAChRs present a possible new drug target for inflammatory disease.

The α4 subunits are among the most common nAChRs contributing to the formation of the high-affinity (α4β2) nicotine-binding sites in cells (Changeux, 2010). In mice lacking the α4 nAChR (α4$^{-/-}$), nicotine binding appears to be all but abolished in several organs (Marubio et al., 1999). The α4 nAChRs are well expressed in immune cells, including T and B lymphocytes, and have been implicated in regulating cytokine release as well as antibody production (Skok et al., 2007). Indeed, α4$^{-/-}$ mice have been found to exhibit abnormalities in lymphocyte development and maturation (Skok et al., 2007).

Because exposure to nicotine appears to up-regulate α4 containing nAChRs in the lymphocytes of human smokers and in rodents (Cormier et al., 2004), we hypothesize an effect of nicotine on immunity. In this study, we show the existence of

This work was supported by Jeffress Memorial Trust [J-953]; a Virginia Youth Tobacco Program grant (to N.K.); and the National Institutes of Health National Institute on Drug Abuse [Grant R01 DA-12610] (to M.I.D.).
dx.doi.org/10.1124/mol.113.088484.
[S] This article has supplemental material available at molpharm.aspetjournals.org.

ABBREVIATIONS: Ab, antibody; BMF, bone marrow fraction; CEMss, human T4 lymphoblastoid cell line; DHβE, dihydro-β-erythroidine; FACS, fluorescence-activated cell sorting; $G\alpha_o$, G protein subunit o; Gprin1, G protein regulated-inducer of neurite outgrowth; ICF, immune cell fraction; ICF_C, immune cell fraction from circulating heart blood; ICF_S, immune cell fraction from spleen; IFN, interferon; IL, interleukin; IP, immunoprecipitation; LC-ESI, liquid chromatograph–electrospray ionization; mAb299, rat monoclonal anti-α4 antibody; MS, mass spectrometry; MSP, mastoparan; nAChR, nicotinic acetylcholine receptor; NF-κB, nuclear factor κB; PBS, phosphate-buffered saline; pEGFP, enhanced green fluorescent protein plasmid; siRNA, small interfering RNA; T_H, helper T cells; WT, wild-type.

an α4 nAChR-expressing population of T lymphocytes ($\alpha4^+$ $CD3^+CD4^+$) in circulation, spleen, bone marrow, and thymus. We demonstrate that nicotine enhances the number of $\alpha4^+$ T cells in these immune organs, leading to a change in cytokine production and release. This mechanism is driven by α4 nAChR signaling via a G protein/CDC42 pathway in T cells.

Materials and Methods

Animals. C57BL6 adult male mice were kept in 12-hour light/dark cycles. The generation of α4 nAChR subunit knockout ($\alpha4^{-/-}$) mice was previously described elsewhere (Ross et al., 2000). For all experiments, the $\alpha4^{-/-}$ mice were backcrossed to at least 10 to 12 generations. The $\alpha4^{-/-}$ and wild-type (WT) mice were obtained from crossing heterozygote mice.

Isolation of the Immune Cell Fraction. An immune cell fraction (ICF) from blood was obtained from the heart via cardiac puncture (Hoff, 2000) and from the spleen and thymus through dissection according to our institutional animal care and use committee regulations. The mice were anesthetized using 5% isoflurane, and the heart, thymus, and spleen were accessed via an abdomen-to-sternum incision. For circulating heart blood (ICF_C), a 1-cc syringe with a 25 1/2 gauge needle was inserted into the left ventricle, and blood was drawn to a volume of 500 μl/mouse. Equal volumes of phosphate-buffered saline (PBS) with 5 mM EDTA was added to the blood fraction as an anticoagulant. Bone marrow fractions (BMF) were obtained by removing the hind leg bones (femur and tibia) and an opening was made to expose the bone marrow. The bone marrow was aspirated out using 0.075M KCl and then incubated at 37°C for 15 minutes before centrifugation at 800*g* to collect the BMF. Tissue dissected from the spleen and thymus was weighed and then homogenized by manual trituration using a sterile Pasteur pipette. The supernatant was centrifuged at 250*g*, and the pellet was resuspended in PBS with 5 mM EDTA. Circulating blood, spleen, and thymus ICF were isolated and pooled using Ficoll-Paque (GE Healthcare Bio-Sciences, Pittsburgh, PA) per the manufacturer's instructions.

Immune Bead Sorting Assay. Immune cells were isolated using a magnetic bead method based on the protocols of Chen et al. (2000) with modifications. For cell isolation, the ICF was preincubated with 10 μg of rat monoclonal anti-α4 antibody (mAb299) (Whiting and Lindstrom, 1988), mouse polyclonal anti-CD4 anitbody (Ab) (Santa Cruz Biotechnology, Dallas, TX), or rabbit IgG Abs (Cell Signaling Technologies, Beverly, MA) in ice-cold PBS for 2 hours before the addition of a precleared Protein G Dynabeads resin (Invitrogen/Life Technologies, Carlsbad, CA). The cells were incubated with the beads for 1 hour, then eluted from the bead matrix by gentle mixing in a 5 μg/ml papain in PBS solution for 15 minutes at room temperature. The papain was inactivated by the addition of RPMI culture media with 5% fetal bovine serum followed by washing in PBS and slow-speed centrifugation (100*g*).

Fluorescence-Activated Cell Sorting. Fluorescence-activated cell sorting (FACS) was conducted using a published protocol (Yoder et al., 2008) with minor modifications. Briefly, $1–2 \times 10^6$ immune cells were pelleted, fixed, and probed with 5 μg of mAb299 and fluorescein isothiocyanate–conjugated CD4 (BD Biosciences, San Jose, CA) for 30 minutes in the dark. Secondary staining was conducted using Dylight 488 (Pierce/Thermo Scientific, Rockford, IL) for 30 minutes in the dark. The cells were washed with PBS then resuspended in a 1% paraformaldehyde fixative before the analysis, which used a FACSCalibur (Becton Dickinson, Franklin Lakes, NJ).

Drug Treatments. The WT and $\alpha4^{-/-}$ mice were given a sustained (6-day) regimen of 0.9% saline or nicotine dissolved in 0.9% saline (0.1–1.5 mg/kg body weight) intraperitoneal injections. The injections were normalized to equal-volume solutions made fresh daily. The nicotine concentrations were based on published studies on chronic drug-associated behaviors (Marubio et al., 2003) and immune effects (Davis et al., 2009). Unless otherwise noted, sustained nicotine treatment is a 6-day treatment. For the cell culture experiments, the human T4 lymphoblastoid (CEMss) cells were exposed to nicotine, nicotine and dihydro-β-erythroidine (DHβE), mastoparan (MSP), or MSP and nicotine (Amin et al., 2003; Nordman and Kabbani, 2012).

Immunocytochemistry and Cell Counting. Cells derived from ICF and CEMss cells were fixed for 15 minutes at room temperature using a solution consisting of 1× PEM (80 mM PIPES, 5 mM EGTA, and 1 mM $MgCl_2$, pH 6.8) containing 0.3% glutaraldehyde. The cells were centrifuged at 1000*g* for 5 minutes then washed with PBS. For G protein regulated-inducer of neurite outgrowth (Gprin1) staining, the cells were permeabilized with 0.1% Triton X-100 before glutaraldehyde quenching using 10 mg/ml sodium borohydride. The cells were blocked in a solution of 10 mg/ml bovine serum albumin + 10% goat serum. Immunostaining was performed using a mouse monoclonal CD3 Ab (Santa Cruz Biotechnology), a mouse monoclonal anti-CD4 Ab (Santa Cruz Biotechnology), a mouse monoclonal CD133 Ab (eBioscience/Affymetrix, San Diego, CA), a rat monoclonal anti-α4 Ab (mAb299) (Whiting and Lindstrom, 1988), a rabbit polyclonal anti-CDC42 Ab (Santa Cruz Biotechnology), a monoclonal mouse anti–active-CDC42 (GTP-CDC42) (NewEast Biosciences, King of Prussia, PA), a rabbit polyclonal anti-Gprin1 Ab (Abcam, Cambridge, MA), a mouse monoclonal anti–β-tubulin Ab (Cell Signaling Technologies), and rhodamine phalloidin (Cell Signaling Technologies). The cells were incubated in anti-rat Dylight 488, anti-mouse Dylight 549, anti-rabbit Dylight 549, and anti-mouse AlexaFluor 647 secondary Abs (Jackson ImmunoResearch Laboratories, West Grove, PA) and mounted in 0.212% n-propyl gallate in 90% glycerol and 10% PBS solution on glass coverslips. Immunostaining was visualized with a Nikon Eclipse 80i confocal microscope fitted with a Nikon C1 CCD camera and a Zeiss. Cell images were captured using an EZ-C1 (Nikon, Melville, NY) camera with AxioVision software (Carl Zeiss, Inc., Thornwood, NY).

For cell counts, the viable cells were counted using a trypan blue (Thermo Fisher Scientific, Waltham, MA) exclusion assay using a C-Chip hemocytometer (INCYTO/Thermo Fisher Scientific) under phase contrast. All cells counts were performed in triplicate, and the data were averaged for each experiment.

Immunohistochemistry and Analysis of Spleen. Spleen extraction and histologic preparation were performed as described elsewhere (Lobato-Pascual et al., 2013). Briefly, adult mice were anesthetized using 5% isoflurane and then perfused using 4% paraformaldehyde, pH 7.2. Spleens were dissected then submerged in the paraformaldehyde solution for 24 hours before being transferred to 30% sucrose. Spleens were embedded in 5% agarose and sectioned in the horizontal plane into 40-μm slices using a vibrating blade microtome (Thermo Fisher Scientific).

For immunohistochemistry, the spleen slices were permeabilized using 0.5% Triton X-100 and quenched by 50 mM ammonium chloride for 30 minutes at room temperature. The tissue was blocked in 10% goat serum then probed with mAb299, a polyclonal anti-Gprin1 Ab (Abcam), a monoclonal anti-CD4 Ab (Santa Cruz Biotechnology), and a monoclonal anti-CD16 Ab (Santa Cruz Biotechnology) overnight at 4°C. Dylight secondary Abs (488 and 549) were used. Intact spleens were mounted onto glass slides using the mounting media described earlier. White and red pulp regions were distinguished by morphology within the intact spleen tissue and in red blood cell enrichment using differential interference contrast imaging.

Cell counts were conducted on fluorescently-labeled sections. For the total cell counts, a total of eight spleen sections were stained with the nucleus label 4′,6-diamidino-2-phenylindole and then counted blindly by 200-μm^2 area. The spleen cell counts were also normalized to the total cells of spleen, which was obtained from hemocytometer analysis relative to the size of the counting area (200 μm^2).

Immunoprecipitation and Western Blot. Membrane protein fractions were obtained after solubilization using a nondenaturing lysis buffer consisting of 1% Triton X-100, 137 mM NaCl, 2 mM EDTA, and 20 mM Tris HCl (pH 8.0) with protease (complete) and phosphatase (σ inhibitor cocktails. This method has been previously found to enable sufficient solubilization of the nAChR from cells and tissue for molecular analysis (Nordman and Kabbani, 2012). For the detection

of protein-protein interaction, immunoprecipitation (IP) using the Protein G matrix (Invitrogen) was performed (Nordman and Kabbani, 2012). Briefly, the IP Ab was bound to a precleared Protein G Dynabead resin, as per manufacturer instructions (Invitrogen). Pure IgG was used to control for nonspecific Ig interaction with the Protein G resin. The IP experiments were performed from ICF preparations at a concentration of 100 μg/ml ICF proteins for Western blot analysis and 750 μg/ml ICF for mass spectrometry (MS) analysis. Experiments were performed in triplicate to ensure a robust result. The primary Abs used for IP and/or Western blotting were mAb299, polyclonal α4 nAChR (Santa Cruz Biotechnology; A-20), polyclonal β2 nAChR (Santa Cruz Biotechnology; H-92), G protein subunit o ($G\alpha_o$) (Santa Cruz Biotechnology), Gprin1 (Abcam), CDC42 (Santa Cruz Biotechnology), GTP-CDC42 (NewEast Biosciences), nuclear factor κB (NF-κB) (Santa Cruz Biotechnology), CD4 (Santa Cruz Biotechnology), and CD16 (Santa Cruz Biotechnology).

Cell Culture. The $CD3^+CD4^+$ CEMss cells were obtained from Dr. Yuntao Wu (George Mason University). The cells were grown in RPMI containing 10% fetal bovine serum and 1% penicillin-streptomycin antibiotic as per published protocols (Yoder et al., 2008). For transfections, human α4 in pcDNA3.1 (provided by Dr. Jerry Stitzel, University of Colorado), Gprin1 in pcDNA3.1 and Gprin1 small interfering RNA (siRNA) in pRNAT H1.1 (provided by Dr. Law, University of Minnesota), and CDC42 in an enhanced green fluorescent protein plasmid (pEGFP)/pcDNA3 (provided by Dr. James Bramburg, Colorado State University) were transfected using Lipofectamine 2000, as described by the manufacturer (Invitrogen). The cells were transfected with 1 μg/cm^2 cDNA for α4, GFP-Gprin1, GFP-CDC42, and pcDNA3-CDC42. Knockdown of Gprin1 was achieved by transfection with 200 pmol/cm^2 of the Gprin1 siRNA in pRNAT H1.1. An empty pEGFP-C1 or pcDNA vector (Addgene, Cambridge, MA) was used as a transfection control.

Enzyme-Linked Immunosorbent Assay Analysis of Cytokine Levels in Plasma and Cultured Cells. An analysis of the cytokines was performed in both the plasma fraction of circulating blood of mice or supernatant from cultured cells. For the collection of blood plasma, we used the Ficoll-Paque separation method as described earlier. For the collection and analysis of cytokines in cultured cells, CEMss cells were treated with nicotine or nicotine and DHβE (for 0, 10, 30, 60, and 120 minutes) and then centrifuged at slow speed (300*g*) for 5 minutes for supernatant collection. Cytokines were recovered using the Ultracel-3 membrane 3 kDa unit (Amicon/Millipore Corp., Billerica, MA). The detection and quantification of IL-6 was conducted using the Rat-Bio enzyme-linked immunosorbent assay Kit Rat IL-6 (R&D Systems, Minneapolis, MN). Detection and quantification of T_H1/T_H2 cytokines was performed using the T_H1/T_H2 enzyme-linked immunosorbent assay Ready-SET-Go! Kit (eBioscience) according to the manufacturer's instructions.

Mass Spectrometry. Liquid chromatography–electrospray ionization (LC-ESI) MS analysis was conducted as described elsewhere (Nordman and Kabbani, 2012). Select bands were manually excised from Coomassie-stained acrylamide gels, then eluted from the gel matrix by alkylation with iodoacetamide, then extracted using trypsin in ammonium bicarbonate. Samples were purified using ZipTips (Millipore Corp., Billerica, MA) before the MS analysis using an LTQ-Orbitrap (Thermo Fisher Scientific). Tandem mass spectra collected by Xcalibur (version 2.0.2; Thermo Fisher Scientific) were searched against the National Center for Biotechnology Information rat protein database using SEQUEST (version 3.3.1; Bioworks Software from Thermo Fisher Scientific). The SEQUEST search results were filtered using the following criteria: minimum X correlation of 1.9, 2.2, and 3.5 for 1+, 2+, and 3+ ions, respectively, and ΔCn >0.1. The protein score represents the X correlation where scores <0.1 were excluded from the analysis. It does not directly reflect the quantity of the protein or peptides in the sample.

Statistical Analysis. Statistical values were obtained using a Student's *t* test or one-way analysis of variance (ANOVA). Asterisks indicate the statistical significance in a Student's *t* test, two-tailed *P* value, ($^*P < 0.05$; $^{**}P < 0.01$; $^{***}P < 0.001$). Error bars indicate S.E.M. All experiments were performed in triplicate, and group averages are presented.

Results

Detection of α4 nAChR Protein Expression in Immune Cells. The nAChRs in immune cells have been identified where they play an important role in cholinergic control of immunity (Kawashima and Fujii, 2003; Skok et al., 2007). To determine the expression of α4 nAChRs, we isolated α4-expressing cells ($\alpha4^+$) from the blood ICF of mice. The ICF is composed primarily of lymphocytes (~30%) and neutrophils (~50%) (Dhabhar et al., 1995). We developed an immunobead cell-sorting assay (hereafter, "bead assay") (Chen et al., 2000) to isolate $\alpha4^+$ cells from ICF (Supplemental Fig. 1). The optimization of the bead assay for the detection of cell surface α4 subunits was performed in human embryonic kidney 293 cells that express $\alpha4\beta2$ receptors (described in Supplemental Fig. 1) (Sallette et al., 2005). Treatment of these cells with papain was found to be negligible on cell number and nAChR expression (Supplemental Fig. 2).

The expression of α4 subunits was confirmed in the $\alpha4^+$ fraction using Western blot analysis (Fig. 1A). Knockout mice lacking the α4 subunit ($\alpha4^{-/-}$) were used as a control for the monoclonal anti-α4 Ab in the assay. A reprobe of the same blot using an anti-β2 Ab shows expression of β2 within the $\alpha4^+$ fraction, consistent with the existence of $\alpha4\beta2$ nAChRs in immune cells (Kawashima and Fujii, 2003).

The $\alpha4^+$ cells were also analyzed using LC-ESI MS (Supplemental Fig. 1). A cluster of differentiation (CD) system was used for immunophenotyping the $\alpha4^+$ cell fraction. A list of CD markers within the $\alpha4^+$ fraction is presented in Supplemental Table 1. A significant number of T cell, B cell, and macrophage cell markers were identified within the $\alpha4^+$ fraction, consistent with previous findings on α4 nAChR expression in various immune cells (Kawashima and Fujii, 2003). In particular, a significant number of T-lymphocyte markers were observed in the $\alpha4^+$ fraction, including the helper T-cell marker glycoproteins CD4, CD28, CCR4, and CXCR3.

Expression of CD4 was confirmed in $\alpha4^+$ cells derived from the bead assay using immunoblotting (Fig. 1A). Our findings verify that a portion of $\alpha4^+$ cells also express CD4 ($\alpha4^+CD4^+$); however, CD4 can also be expressed on macrophages and dendritic cells, so we probed the $\alpha4^+$ fraction with a CD16 Ab to assess the level of macrophage, neutrophil, and natural killer cells. As shown in Fig. 1A, the CD16 expression was lower than CD4 expression in the $\alpha4^+$ fraction, suggesting that the majority of α4 receptors are on T cells.

FACS and immunocytochemistry were used to further characterize $\alpha4^+$ cells in ICF. Similar to previous studies (Darsow et al., 2005), the $\alpha4^+$ cells were isolated by FACS and found to constitute 3.9% of the total ICF (Fig. 1B). The FACS experiments from $\alpha4^{-/-}$ mice show a <0.1% detection of the Ab signal (Supplemental Fig. 2C). FACS was also used to analyze $\alpha4^+$ cells isolated from the ICF using the bead assay (Supplemental Fig. 1). $CD4^+$ cells accounted for 23.0% of the $\alpha4^+$ population (Fig. 1C), which was consistent with earlier findings on CD4 expression (Fig. 1A).

Cell suspensions of ICF were stained with anti α4 nAChR, CD3, and CD4 Abs. As shown in Fig. 1D and Supplemental Fig. 2D, immunolabeling shows a noticeable portion of the

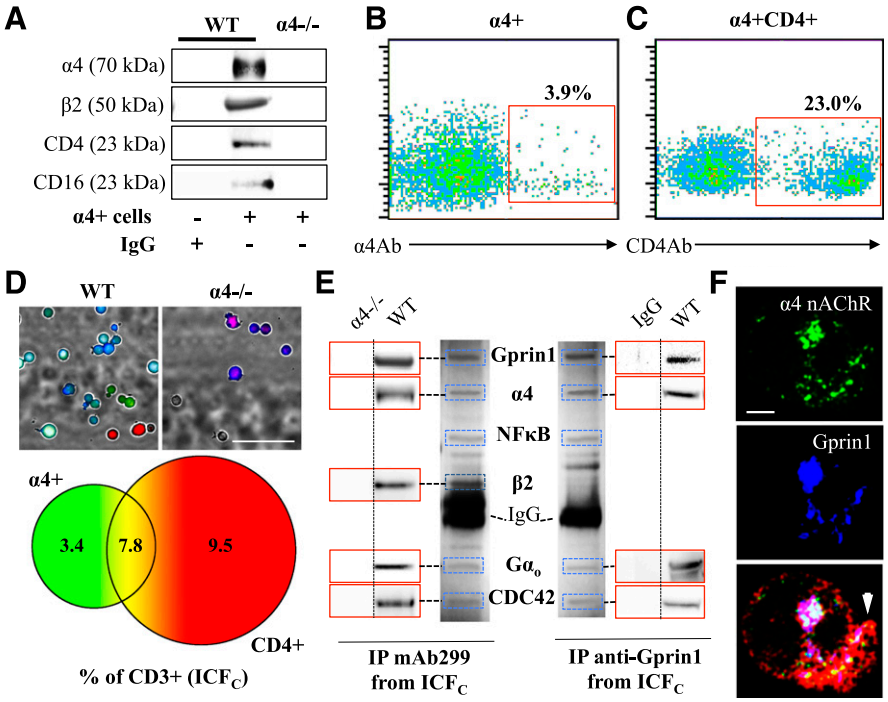

Fig. 1. Isolation of α4 nAChRs and their signaling partners in CD4+ cells. (A) Western blot detection of α4 and β2 nAChRs, CD4, and CD16 within the α4+ fraction isolated from ICF_C using the bead assay (n = 3 mice for WT and $\alpha4^{-/-}$). IgG beads (+ lane) and ICF_C from $\alpha4^{-/-}$ mice (right lane) were used as controls. (B) FACS immunosorting of α4+ cells from ICF_C (n = 3 mice). (C) The α4+ population from B was separated using an anti-CD4+ Ab (n = 3 mice). (D) Immunocytochemical detection of α4 nAChR (green), CD4 (red), and CD3 (blue) within the ICF_C. Fluorescent signals are overlaid on differential interference contrast images. The diagram shows the proportion of stained cells in the CD3+ ICF_C (n = 3 mice). Scale bar: 50 μm. (E) A Coomassie-stained gel showing the position of bands (blue boxes) analyzed by LC-ESI MS within α4 nAChR and Gprin1 IP experiments from ICF_C. The $\alpha4^{-/-}$ ICF and IgG Abs were used as a negative control for the IP. MS results are presented in Supplemental Tables 2 and 3. Western blot confirmation of the interaction is shown in red boxes (n = 3 mice). (F) Colocalization of α4 nAChRs, Gprin1, and phalloidin (red) in a CD4+ cell isolated using the bead assay. The bottom image shows the expression of the proteins in actin-rich domains (arrow). Scale bar: 1 μm.

ICF population cells expressing α4, CD4, and CD3 proteins. Moreover, ~7.8% of the CD3+ ICF population were found to coexpress α4 and CD4 proteins, confirming the existence of an α4 nAChR T-cell population in blood. ICF from $\alpha4^{-/-}$ did not show strong immunoreactivity to the α4 Ab in the analysis (Fig. 1D), supporting the specificity of the mAb299 in the experiment.

Characterization of an α4 nAChR Signaling Apparatus in Immune Cells. Receptors are components of large protein complexes (interactomes) underlying the mechanisms of receptor signaling and regulation in cells (Kabbani et al., 2007). To explore interactions of the α4 nAChR, we coupled coimmunoprecipitation and LC-ESI MS (Nordman and Kabbani, 2012) to define α4 nAChR interacting proteins in immune cells (Supplemental Fig. 1). In these experiments, ICF from $\alpha4^{-/-}$ mice were used as a negative control for the immunoprecipitating anti-α4 nAChR Ab (mAb299). As shown in Fig. 1E, an interaction network comprising Gprin1, $G\alpha_o$, the β2 nAChR subunit, and CDC42 was detected within the immunoprecipitated α4 nAChR complex from ICF. The presented gel reveals the position of protein bands coimmunoprecipitated with the α4 nAChR. The identity of the proteins was confirmed using MS peptide analysis (Supplemental Table 2) and Western blotting (Fig. 1E). Gprin1 and $G\alpha_o$ have been shown to bind nAChRs in neural cells (Nordman and Kabbani, 2012), suggesting that the interactions are common to neural and immune cells.

Gprin1 has been found to regulate the signaling and localization of opioid and nAChRs (Ge et al., 2009; Nordman and Kabbani, 2012). We validated interactions between α4 nAChRs and Gprin1 in immune cells by immunoprecipitating Gprin1 from the ICF and identifying the components of its interactome using the same proteomic approach. IgG was used as a negative control for immunoprecipitation. We have used Gprin1 Abs for immunoprecipitation studies (Nordman and Kabbani, 2012). As shown in Fig. 1E, Gprin1 and α4 nAChRs share common binding partners in immune cells. Coexpression of α4 and Gprin1 was verified in CD4+ cells using an anti-CD4 bead assay. Immunostaining of these cells with α4 and Gprin1 Abs demonstrates coexpression of the proteins in immune cells and their colocalization at f-actin-rich membrane domains (Fig. 1F).

α4 nAChRs Regulate CD4+ T-Cell Proliferation. CD4+ cells play an important role in immune function by supporting the activity of B-cells and macrophages (Itano and Jenkins, 2003). We assayed the expression and interaction of α4 nAChRs within ICF_C, spleen (ICF_S), and thymus (ICF_T). As shown in Fig. 2A, immunoreactivity for α4 nAChRs, CD4, and Gprin1 was detected in all three fractions ($ICF_{C/S/T}$). We used glyceraldehyde 3-phosphate dehydrogenase as a loading control. Studies have indicated an effect of chronic nicotine on cytokine and Ab production (Song et al., 1999; Skok et al., 2007). We examined the effects of a 6-day (sustained) nicotine treatment (0.5–1.0 mg/kg) in mice. Nicotine injections were also performed in $\alpha4^{-/-}$ mice. A dose-dependent increase in spleen and thymus weight was observed in response to nicotine treatment in WT mice (Fig. 2B; Supplemental Figs. 3 and 4). Nicotine did not dramatically alter the size of the spleen or thymus in $\alpha4^{-/-}$ mice, suggesting that α4 expression is necessary for the effect.

Next, we quantified cells in the $ICF_{C/S/T}$. Consistent with its effect on organ size, nicotine was found to increase the cell number in a dose-dependent manner at the tested doses of 0.1–1.5 mg/kg body weight in the $ICF_{C/S/T}$ of mice (Fig. 2C; Supplemental Fig. 3B and 4B). We did not detect a change in cell number in $\alpha4^{-/-}$ mice in response to nicotine (Fig. 2C). To examine the cell-specific effects of nicotine, we analyzed the ICF_S by FACS. Nicotine was found to increase $\alpha4^+$ cells by 4.8%, $\alpha4^+CD4^+$ cells by 7.1%, $CD4^+$ cells by 5.1%, and $CD3^+CD4^+$ cells by 1.9% (Fig. 2D). A similar analysis of ICF_S from $\alpha4^{-/-}$ mice exposed to nicotine showed a negligible rise in $CD4^+$ cells (0.4%) and $CD3^+CD4^+$ cells (0.4%) (Fig. 2D),

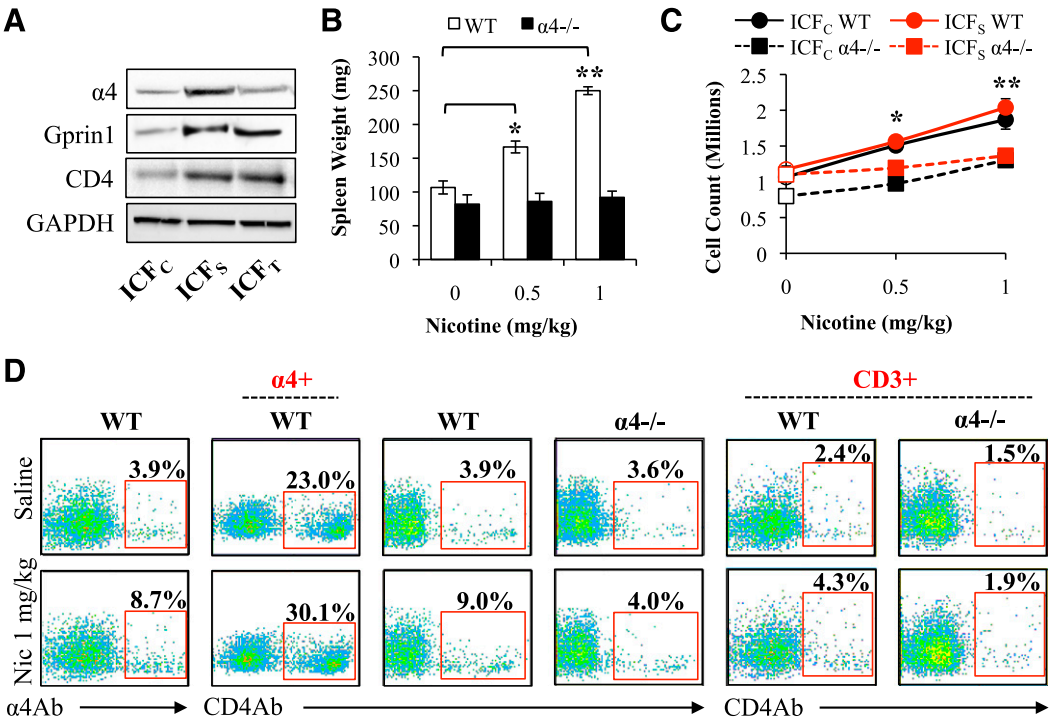

Fig. 2. Nicotine promotes immune-cell proliferation via the $\alpha 4$ nAChR. (A) Western blot detection of $\alpha 4$, Gprin1, CD4, and glyceraldehyde 3-phosphate dehydrogenase (GAPDH) in the ICF. Each lane was loaded with 100 μg of protein (n = 3 mice). (B) Changes in spleen weight in WT and $\alpha 4^{-/-}$ mice injected with 0.5 or 1.0 mg/kg nicotine daily for 6 days or vehicle (saline) (n = 3 mice for WT and $\alpha 4^{-/-}$). (C) Total counted cells in ICF_C and ICF_S of nicotine-treated mice (n = 3 mice/condition for WT and $\alpha 4^{-/-}$). (D) FACS separation of the ICF from nicotine and saline-treated mice (n = 3 mice/condition for WT and $\alpha 4^{-/-}$). A bead assay was used to isolate $\alpha 4^+$ and $CD3^+$ cells (red) before FACS analysis with an anti-CD4 Ab. *$P < 0.05$; **$P < 0.01$.

suggesting that $\alpha 4$ nAChRs contribute to nicotine-mediated T-cell proliferation.

α4- and Gprin1-Expressing Helper T Cells Respond to Nicotine. Studies show that nAChRs play a role in immune function in the spleen (Tracey, 2009). We have determined an expression of $\alpha 4$ nAChRs in immune cells of spleen, thymus, and circulation (Fig. 2A). Next, we immunohistochemically examined the distribution of $\alpha 4$ nAChRs and Gprin1 in the spleen. Cells were also labeled with the helper T-cell marker CD4 or the macrophage, neutrophil, and natural killer marker CD16.

The spleen is divided into two main compartments: white pulp, which is abundant in T and B lymphocytes, and red pulp, which is abundant in red blood cells and macrophages (Barnhart and Lusher, 1976). As shown in Fig. 3A, Gprin1 immunolabeling was seen in both red and white pulp regions. The $\alpha 4^+CD4^+$ expression, on the other hand, appeared localized to the white pulp (Fig. 3A), consistent with the role of $\alpha 4$ nAChRs in T-cell function. A quantitative assessment of the immunolabeling indicates that the majority of $\alpha 4^+CD4^+$ cells also express Gprin1 (Fig. 3, A and C) and CD3 (data not shown). A subset of $CD16^+$ cells was also found to stain for Gprin1 (data not shown).

Human smoking is associated with spleen disorders such as extramedullary hematopoiesis (Pandit et al., 2006) and splenomegaly (Kupfer, 1992). We explored the effect of nicotine on T-cell proliferation in the spleen. As indicated in Fig. 3, B and C, nicotine was found to augment the percentage of $\alpha 4^+$ (+4.4%) and $CD4^+$ (+2.4%) cells in the white pulp relative to the total cell counts per the same 200 μm^2 area. Nicotine was also found to increase the ratio of $\alpha 4^+CD4^+$ $Gprin1^+$ cells in the spleen (+1.9%) (Fig. 3C). This finding was confirmed by staining the ICF_S, which showed a 3% rise in the $\alpha 4^+CD4^+Gprin1^+$ cell population (Fig. 3D) in response to nicotine. Experiments in $\alpha 4^{-/-}$ mice show that nicotine only marginally increases the $CD4^+$ cell number (+1.1%, data not shown), underscoring the role of $\alpha 4$ nAChRs in the process.

T-cell proliferation is associated with changes in cytoskeletal signaling (Muller et al., 2006). We explored the effect of nicotine on the localization of $\alpha 4$ nAChRs and Gprin1 in $CD4^+$ cells from the ICF_S of nicotine-treated mice. The specificity of anti-$\alpha 4$ Ab (mAb299) was tested in $\alpha 4^{-/-}$ mice (Figs. 1, D and E, and 3B). The specificity of anti-Gprin1 Ab in immunocytochemical analysis was tested in cultured T cells, which showed a correlation between the Ab signal and Gprin1 expression in the cell (Supplemental Fig. 5). As shown in Fig. 3E, nicotine was found to alter the distribution of $\alpha 4$ nAChRs and Gprin1 in $CD4^+$ cells. In particular, nicotine promoted a translocation of Gprin1 from the cytosol to the plasma membrane in dividing cells (Fig. 3E). In $CD4^+$ cells of $\alpha 4^{-/-}$ mice, nicotine did not alter Gprin1 expression.

Nicotine Promotes Proliferation of $\alpha 4^+$/$Gprin1^+$/$CD4^+$ Cells in Bone Marrow. To determine the effect of nicotine on T-cell proliferation in the bone marrow, mice were injected with nicotine (0.5 and 1.0 mg/kg) for 6 days. Consistent with its effects in the $ICF_{C/S/T}$, nicotine also increased the total number of cells in the BMF (Fig. 4A). Because smoking has been shown to influence hematopoiesis (Pandit et al., 2006; Chang et al., 2010), the BMF was immunolabeled for $\alpha 4$, Gprin1, CD4, and the hematopoietic stem cell marker CD133 (Yin et al., 1997). As shown in Fig. 4, B and C, $\alpha 4^+$ cells in the BMF were found to

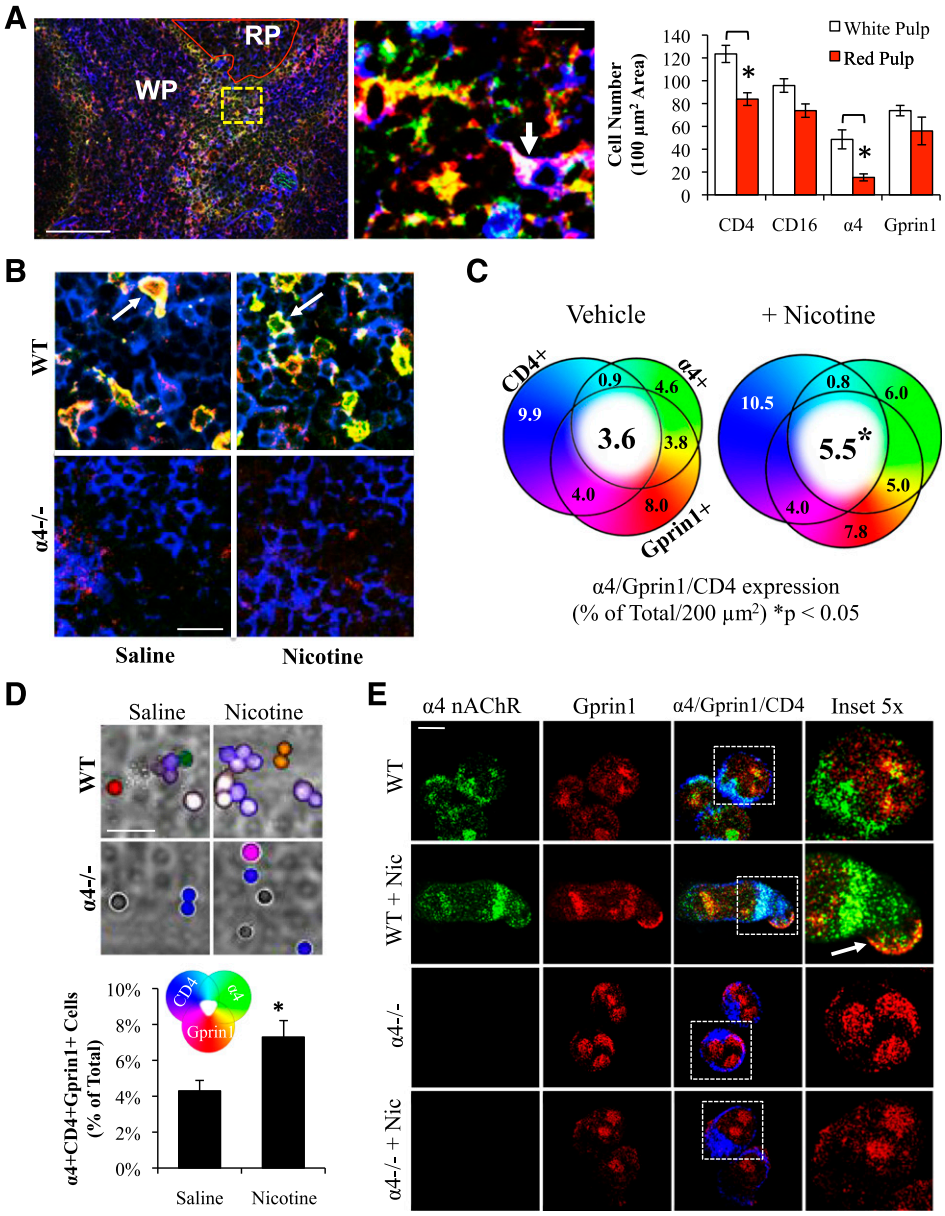

Fig. 3. Nicotine promotes proliferation of $\alpha4^+CD4^+Gprin1^+$ cells in the spleen. (A) Immunohistochemical analysis of $\alpha4$ nAChRs (green), Gprin1 (red), and CD4 (blue) in spleen (n = 3 mice). $\alpha4$, Gprin1, CD16, and CD4 expressing cells were quantified in the white pulp and red pulp regions. Triple immunolabeling (arrow) was seen in the white pulp. Scale bars: 50 μm; 5 μm (magnified image). (B) Images of the white-pulp immunostained as in A. Spleens were obtained from WT and $\alpha4^{-/-}$ mice injected with nicotine or saline for 6 days. Arrows point to $\alpha4^+CD4^+Gprin1^+$ cells. Scale bar: 5 μm. (C) Percentage of cells expressing $\alpha4$, Gprin1, and CD4 in spleen from total per 200 μm^2 area (n = 3 mice/condition for WT and $\alpha4^{-/-}$). (D) Quantification of $\alpha4$ nAChRs (green), Gprin1 (red), and CD4 (blue) expression in cell suspension of the ICF_S from WT and $\alpha4^{-/-}$ mice treated with nicotine or saline (n = 3 mice/condition for WT and $\alpha4^{-/-}$). Fluorescent signals are overlaid over differential interference contrast image. Scale bar: 10 μm. (E) Localization of $\alpha4$ nAChR (green), Gprin1 (red), and CD4 (blue) in cells (same as D). Inset shows colocalization of $\alpha4$ and Gprin1 in $CD4^+$ cells. Nicotine was found to promote $\alpha4$ and Gprin1 expression at the cell surface and periphery (arrow). Scale bar: 1 μm. *P < 0.05.

express $CD4^+$ or $CD133^+$ proteins. Most $\alpha4^+$ cells were also immunoreactive for the anti-Gprin1 Ab (Fig. 4, B and C), which was detected throughout the BMF (data not shown). Treatment with nicotine was found to increase the number of $\alpha4^+Gprin1^+$ cells in the BMF, but this effect was not found to be statistically significant (saline: 25% of total [±4%]; 0.5 mg/kg nicotine: 27% of total [± 4%], $P = 0.54$; 1.0 mg/kg nicotine: 31% [±3%], $P = 0.23$). Consistent with findings in the spleen (Fig. 3C), nicotine was found to significantly enhance the number of $\alpha4^+Gprin1^+$ $CD4^+$ cells and in a dose-dependent manner (Fig. 4, C and D). In contrast, nicotine treatment was found to decrease the overall number of $\alpha4^+Gprin1^+CD133^+$ cells in the BMF, suggesting that nicotine may promote stem cell proliferation.

α4 nAChRs Signal via CDC42 in T Cells. Although nAChRs are known to play an important role in immune function (Tracey, 2009), little is known about their intracellular signaling in immune cells. We used a human T4-lymphoblastoid cell line, CEMss ($CD3^+CD4^+$) to elucidate $\alpha4$ nAChR signaling in T cells (Yoder et al., 2008). This T-cell line also endogenously expresses $\alpha4$ and $\beta2$ nAChRs as well as Gprin1 (Fig. 5A), enabling the study of this pathway endogenously. An IP of the $\alpha4$ nAChR validated interaction between the $\alpha4\beta2$ nAChR and Gprin1 (Fig. 5A). Nicotine and ACh are mitogenic agents in some immune cells (Hawkins et al., 2002). Similar to our observations on $CD4^+$ cells in vivo (Fig. 2), we found that nicotine significantly promotes proliferation of CEMss cells. As shown in Fig. 5B, nicotine treatment was associated with a dose-dependent increase in T-cell number that was abolished by the $\alpha4\beta2$ nAChR specific-antagonist DHβE.

CDC42, a rho GTPase, can mediate actin polymerization leading to changes in cytokine release and T-cell division (Guo et al., 2010). $G\alpha_o$ and Gprin1 have been shown to regulate CDC42 activity in neural cells (Nakata and Kozasa, 2005), and $G\alpha_o$ is found to also regulate CDC42 in T cells (Garcia-Bernal et al., 2011). Based on the discovery of an interaction

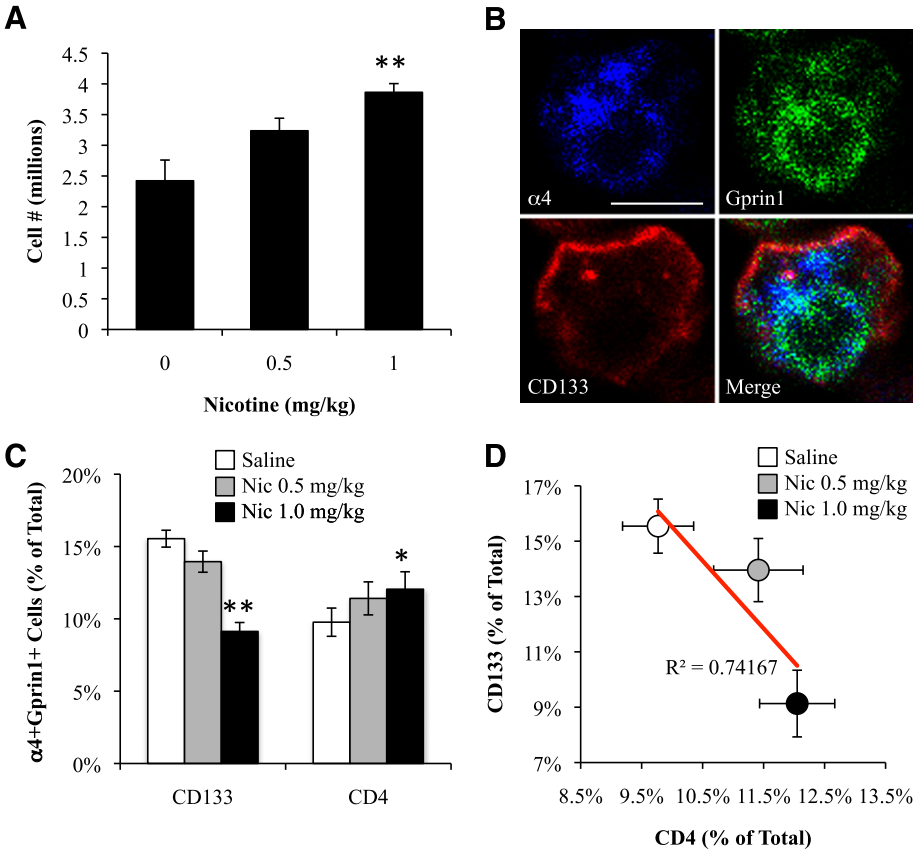

Fig. 4. Nicotine promotes proliferation of $\alpha4^+CD4^+Gprin1^+$ cells and differentiation of $\alpha4^+CD133^+Gprin1^+$ in the bone marrow. (A) Total counted cells in BMF of nicotine-treated mice (n = 3 mice/condition for WT and $\alpha4^{-/-}$). (B) Localization of $\alpha4$ nAChR (blue) and Gprin1 (green) in $CD133^+$ (red) stem cells. (C) Percentage of cells expressing $\alpha4$, Gprin1, and CD4/CD133 from bone marrow (n = 3 mice/condition for WT and $\alpha4^{-/-}$). (D) A comparison of $CD4^+$ versus $CD133^+$ expression in $\alpha4$/Gprin1-expressing cells. $^*P < 0.05$; $^{**}P < 0.01$.

between $\alpha4$ nAChRs, Gprin1, $G\alpha_o$, and CDC42 (Fig. 1E), we hypothesized that $\alpha4$ nAChRs operate via a Gprin1 pathway to regulate CDC42 in T cells. To test this, CEMss cells were transiently transfected with Gprin1 (pcDNA3.1), Gprin1 RNAi (pRNAT H1.1), or CDC42 (pEGFP) expression vectors.

Preliminary studies showed that transfection of these cells with constructs encoding Gprin1 and CDC42 increases their respective protein levels by 108 and 94%, respectively. Transfection with Gprin1 siRNA reduces Gprin1 protein expression by 87% (Supplemental Fig. 5). As shown in Fig. 5C, nicotine had little or no effect on T-cell proliferation in cells overexpressing Gprin1 or CDC42. In contrast, T-cell proliferation was significantly enhanced after transfection with Gprin1 siRNA and nicotine treatment. Indeed, even in the absence of nicotine, Gprin1 siRNA was found to increase T-cell number by 52% (data not shown). Involvement of $G\alpha_o$ was established by examining the effects of the $G\alpha_o$-activator MSP on nicotine treatment (Yamauchi et al., 2000). As shown in Fig. 5C, nicotine did not effect T-cell proliferation in the presence of MSP, confirming a role for $G\alpha_o$ in the pathway. These results suggest that Gprin1 inhibits (nicotine-mediated) T-cell proliferation, possibly via the negative regulation of CDC42.

T-cell proliferation and cytokine release are mediated by GTP activation of CDC42 (Su et al., 2005). Using an Ab selective for CDC42 in the GTP-bound state (GTP-CDC42) we determined the effect of nicotine on CDC42. CDC42 was found in T cells and appeared to colocalize with Gprin1 in actin-rich domains (Fig. 5D). We found a dose-dependent reduction in GTP-CDC42 expression after nicotine treatment (Fig. 5E) and detected an effect at levels below its EC_{50}, suggesting that low levels achieved by smokers (<1 μM) (Russell et al., 1980) contribute to immunity. The effect of nicotine was abolished by DHβE, confirming the role of $\alpha4\beta2$ nAChRs in CDC42 activation. A similar effect of nicotine on CDC42 was observed in vivo. GTP-CDC42 expression was significantly reduced in ICF_s of mice treated with nicotine, and a small increase in GTP-CDC42 levels was observed in nicotine-treated $\alpha4^{-/-}$ mice (Fig. 5F). The total CDC42 levels appeared unaltered (data not shown).

The involvement of Gprin1 in the activation of CDC42 was also tested. As shown in Fig. 5G, a knockdown of Gprin1 protein expression (via siRNA) was found to decrease CDC42 activation (−90% GTP-CDC42 levels) in the cell. In T cells with reduced Gprin1, nicotine did not affect the GTP-CDC42 levels, suggesting that Gprin1 is necessary for nicotine-mediated CDC42 regulation. This is consistent with the results showing that overexpression of CDC42 in the cell is sufficient to override the effects of Gprin1 siRNA on GTP-CDC42 levels (Fig. 5G), which indicates that CDC42 is regulated downstream of Gprin1 in the pathway. Taken together, the data present a new mechanism of $\alpha4$ nAChR signaling in T cells involving Gprin1 modulation of CDC42.

Nicotine Promotes T_H2 Immunity via the $\alpha4$ nAChR. Helper T cells play an important role in mediating the immune response via the distinct actions of T_H1 and T_H2 cell types (Cocks et al., 1995). A change in the T_H1/T_H2 ratio has been examined via detection of cell surface markers such as the chemokine receptors CXCR3 [chemokine (C-X-C motif) receptor 3] and CCR4 [C-C chemokine receptor type 4] as well as the release of specific cytokines (Cocks et al., 1995). Nicotine has previously been found to promote a T_H2 immune response in CD4 T cells (Zhang and Petro, 1996). We examined the role

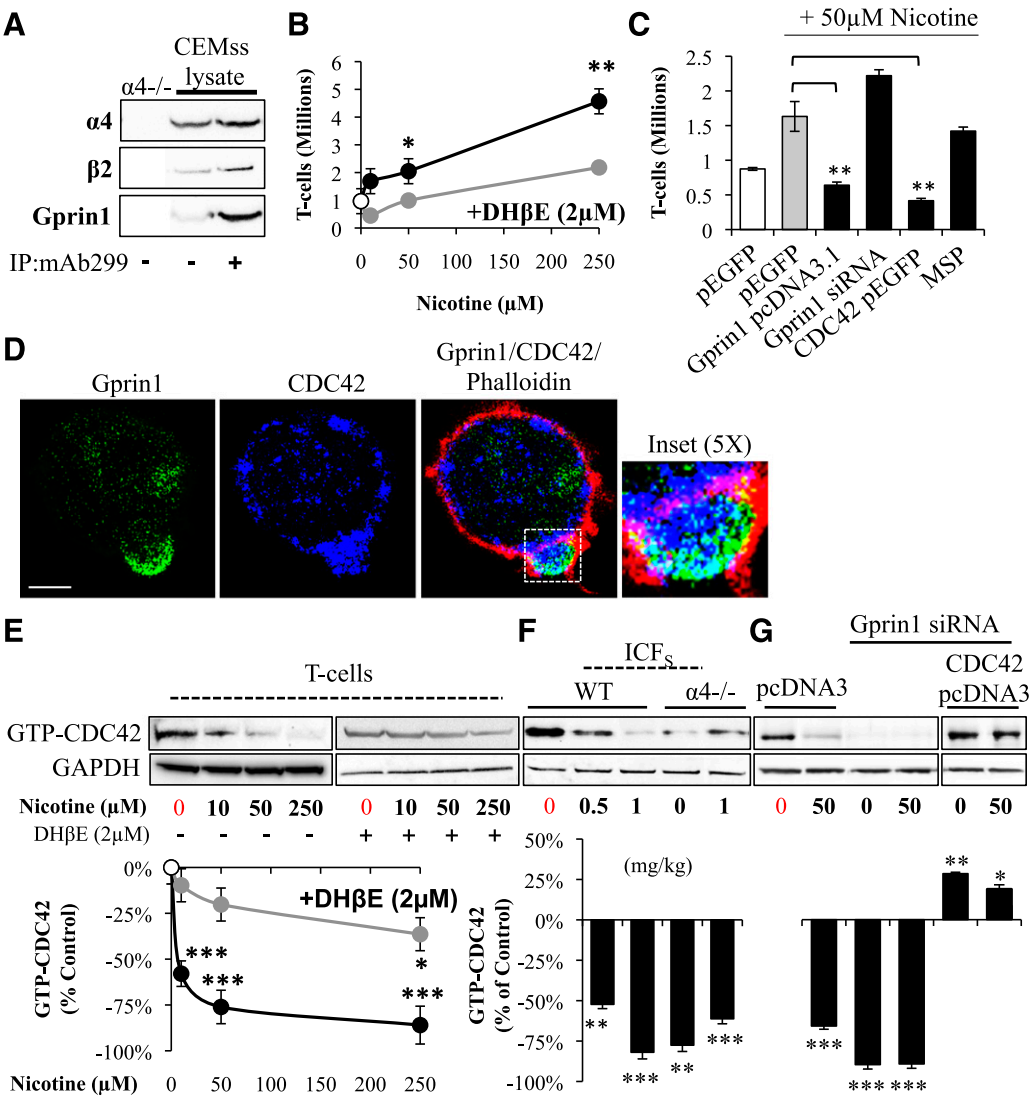

Fig. 5. α4 nAChRs regulate proliferation via a Gprin1/Gα_o/CDC42 pathway. (A) Detection and IP of α4, β2, and Gprin1 complexes in CEMss cells (n = 3 mice for $\alpha4^{-/-}$ and n = 3 separate experiments for CEMss). [−] lane: no Ab control. (B) Cell counts in response to nicotine treatment or nicotine and (2 μM) DhβE (n = 3 separate experiments/condition). (C) Changes in T-cell number after transfection of Gprin1, Gprin1 siRNA (pRNAT H1.1), CDC42 (pEGFP), or treatment with 30 μM MSP (n = 3 separate experiments/condition). An empty pEGFP vector was used as a transfection control. (D) Colocalization of Gprin1 and CDC42 in a CEMss cell. Cells were also stained with rhodamine phalloidin (red). Scale bar: 1 μm. (E–G) Western blot analysis of GTP-CDC42. Average percentage change in GTP-CDC42 relative to control groups (red) (n = 3 separate experiments/condition). (E) CEMss cells (T cells) treated with nicotine or nicotine and DhβE (n = 3 separate experiments/condition). (F) ICF$_S$ from mice treated with saline or nicotine for 6 days (n = 3 separate trials/condition). (G) CEMss cells transfected with Gprin1 siRNA (pRNAT H1.1), CDC42 cDNA (pcDNA3), or an empty (pcDNA3) vector before drug treatment (n = 3 separate experiments/condition). GAPDH, glyceraldehyde 3-phosphate dehydrogenase. *$P < 0.05$; **$P < 0.01$; ***$P < 0.001$.

of α4 nAChRs in the nicotine-associated immune response of T-cells.

As shown in Fig. 6, a significant increase in the level of T_H2 cytokines (IL-4, IL-6, and IL-10) was detected in mice treated with nicotine for 6 days. In comparison, nicotine had little effect on T_H1 cytokine [interferon-γ (IFN-γ) or IL-2] levels (Fig. 6). Because the cytokine levels did not change in $\alpha4^{-/-}$ mice after sustained nicotine treatment, we presume the α4 nAChR to be necessary for these T_H2 responses.

We assessed cytokine release in cultured T cells. CEMss cells were treated with nicotine (0–120 minutes) and then analyzed for IFN-γ, IL-2, IL-4, IL-6, and IL-10 release. As shown in Fig. 6, nicotine treatment significantly increased T_H2 cytokine release from T cells but failed to do so in the presence of DhβE (which was also found to decrease IL-4 release from the cell). We also found that nicotine attenuated the levels of the T_H1 cytokine IFN-γ released from T cells, and this effect was also abolished by DhβE (Fig. 6). IL-2 release, however, appeared unaffected by nicotine treatment, suggesting that α4 nAChRs regulate the release of T_H2 cytokines from T cells.

An α4 nAChR Signaling Mechanism for IL-6 Release from T Cells. IL-6 has been shown to promote a T_H2 response via activation of immature helper T cells (Diehl and Rincon, 2002). We hypothesized that α4 nAChR regulates IL-6 release via the Gprin1/CDC42 pathway. To test this, we examined the effects of Gprin1 and CDC42 overexpression as well as Gprin1 knockdown on IL-6 release after nicotine treatment.

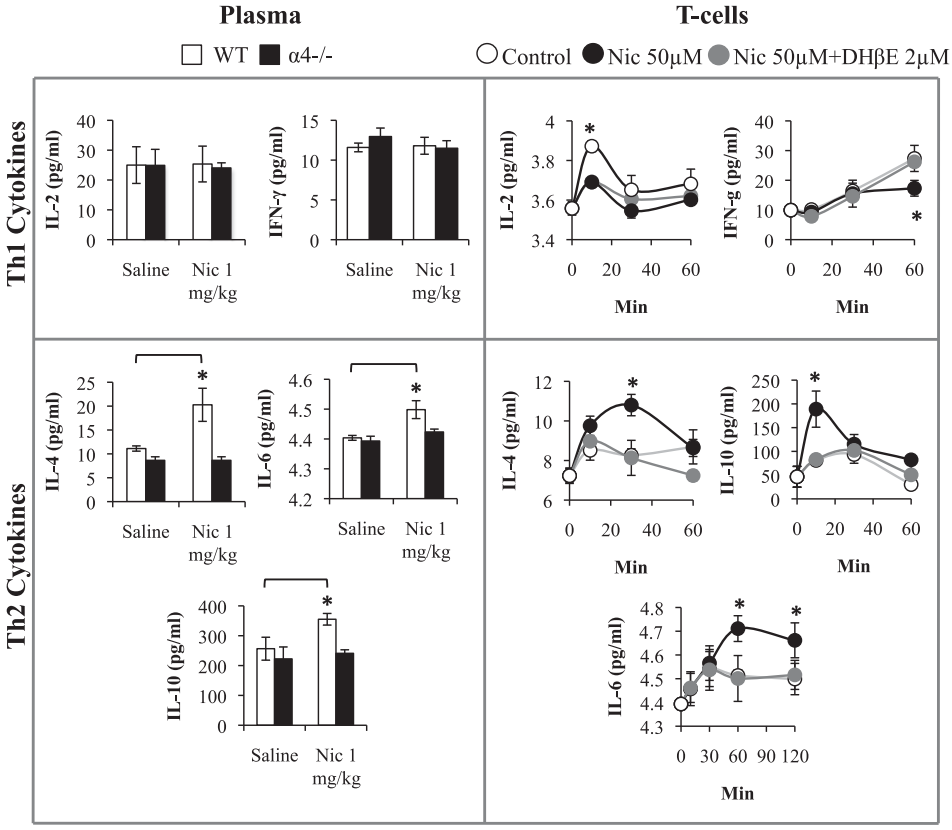

Fig. 6. Nicotine promotes an increase in T_H2 cytokines. Detection of T_H1 and T_H2 cytokines in the plasma of mice and the supernatant of cultured CEMss T cells (n = 3 mice/condition for WT and $\alpha4^{-/-}$ and $n = 3$ separate experiments/condition for CEMss). A significant increase in the level of T_H2 cytokines was detected in mice treated with nicotine for 6 days as well as CEMss cells exposed to a 0–120 minutes nicotine time course. CEMss cells were also analyzed for T_H1 and T_H2 cytokine release in the presence of nicotine and (2 μM) DHβE. *$P < 0.05$.

As shown in Fig. 7A, nicotine was found to increase IL-6 release from T cells, consistent with earlier reports (Kondo et al., 2010) and our observations in vivo (Fig. 6). In response to nicotine, the cells transfected with cDNA for Gprin1 or CDC42 did not present an increase in IL-6 release compared with controls, whereas cells transfected with Gprin1 siRNA appeared to release more IL-6, suggesting that Gprin1 inhibits cytokine production/release in the presence of nicotine.

To determine whether the synthesis of IL-6 was affected, we performed immunoblot analysis of the total IL-6 expression in T cells. As shown in Fig. 7B, IL-6 production increased in response to nicotine, consistent with the data on IL-6 release. In cells transfected with Gprin1 siRNA, IL-6 levels also increased, revealing an effect of Gprin1 on cytokine production as well as release. Transfection of cells with Gprin1 or CDC42 cDNA as well as treatment with nicotine in the presence of DHβE appeared to decrease IL-6 production (Fig. 7B) as it did for release. These results demonstrate that IL-6 production and release are coupled in T cells and that $\alpha4$ nAChR signaling via Gprin1 and CDC42 regulates cytokine production and release. In particular, Gprin1 and CDC42 appear to block the production and release of IL-6 from T cells.

We imaged CEMss cells for IL-6 expression in the presence and absence of nicotine. As expected, nicotine was found to augment the expression of IL-6 (+31.1%) in T cells (Fig. 7, C and D). Specifically, nicotine was found to enhance IL-6 expression in vesicle-like structures and to promote its localization at tubulin- and actin-rich regions of the plasma membrane (Fig. 7C), suggestive of enhanced released.

Nicotine-mediated IL-6 expression was diminished by the addition of DHβE, resulting in a decrease in the immunofluorescence and Western blot signal of IL-6 in T cells (Fig. 7, B–D). Cell image data strongly corroborate the biochemical findings in these studies, highlighting a role for $\alpha4$ nAChR in IL-6 localization and possible release. Finally, involvement of Gprin1 in $\alpha4$ nAChR signaling was established by the finding that Gprin1 overexpression diminishes the number of IL-6–expressing cells (−9.5%) and IL-6 fluorescence within vesicle-like structures (−14.8%), even in the presence of nicotine (Fig. 7, C and D).

Discussion

The immune system functions to modulate inflammation and stress responses throughout the body (Rius et al., 2008). The contributions of nAChRs to immunity have emerged well after the discovery of nAChR expression in immune cells over 30 years ago (Lennon, 1976). In this study, we have shown that nicotine promotes $CD4^+$ T-cell function via the $\alpha4$ nAChR. Although cigarette smoke contains more than just nicotine, the observed effects of nicotine in this study advocate an important role for this substance on T-cell driven immunity (Sopori, 2002). Thus, $\alpha4$ nAChRs may play a central role in the actions of nicotine on T cells and inflammation, leading to an increased susceptibility to immune diseases such as Crohn's disease and rheumatoid arthritis (Sopori, 2002). Interestingly, these same receptors may also contribute to the protective effects of nicotine in conditions such as ulcerative colitis and Parkinson's disease (Guslandi, 1999; Quik et al., 2012).

Nicotine Promotes T_H2 Immunity via the $\alpha4$ nAChR. The lack of electrophysiologic data on nAChR function in

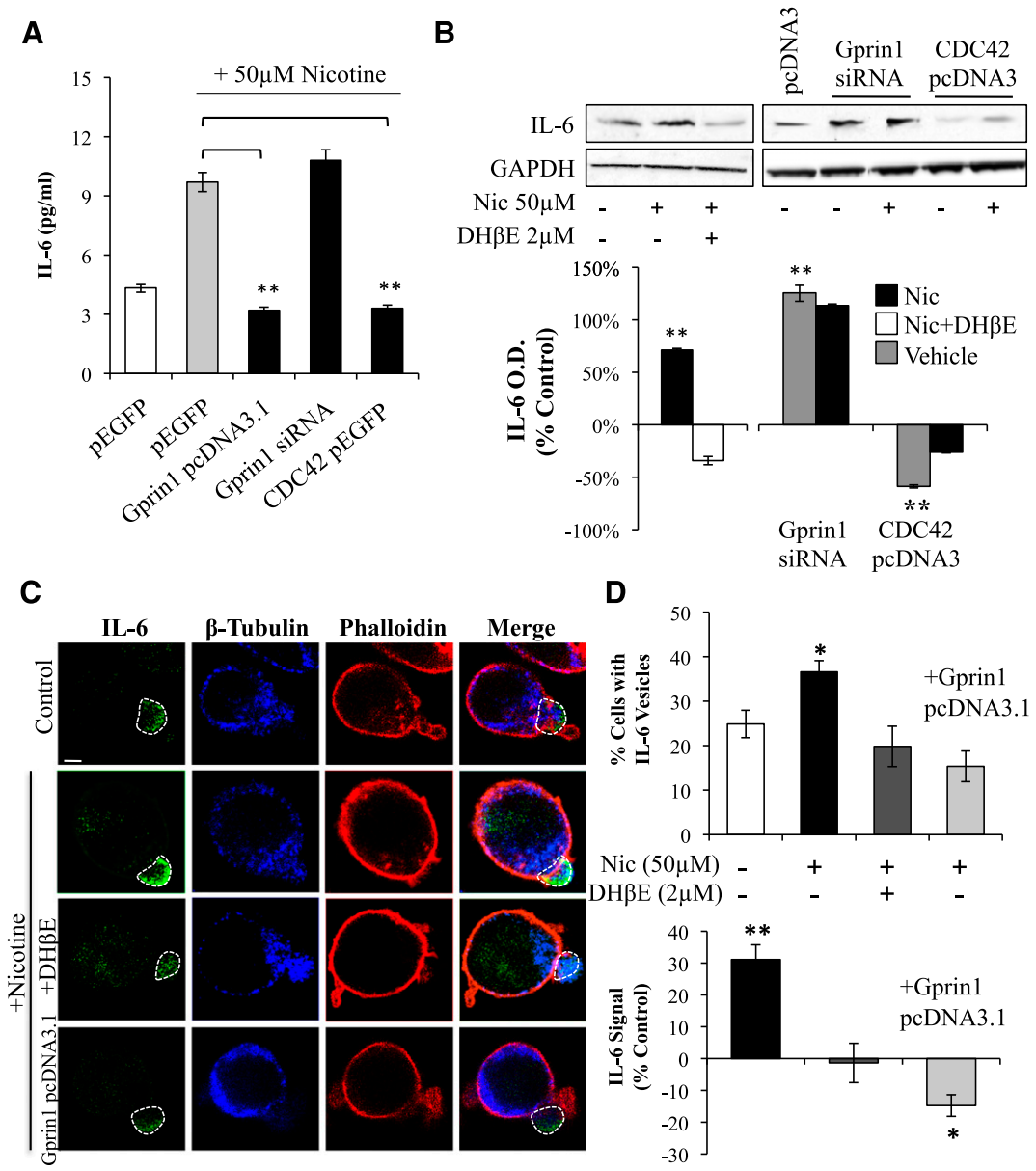

Fig. 7. α4 nAChR signaling via the Gprin1/CDC42 pathway promotes IL-6 release from T cells. (A and B) Transfected cells were analyzed for IL-6 release via an enzyme-linked immunosorbent assay (A) or a Western blot (B) (n = 3 separate experiments/condition). (C) Detection of IL-6 and cytoskeletal proteins in CEMss cells. Bottom row: CEMss cells transfected with Gprin1 pcDNA3.1 before nicotine (Nic) treatment. Scale bar: 1 μm. (D) The percentage of cells expressing IL-6 and relative percentage of the signal within T cells (indicated ROI in C) (n = 3 separate experiments/condition). GAPDH, glyceraldehyde 3-phosphate dehydrogenase. *$P < 0.05$; **$P < 0.01$.

immune cells has stymied explanations of their contributions to immunity. Signaling through α7 nAChRs has been found to attenuate the production of cytokines such as tumor necrosis factor α in monocytes and macrophages contributing to the parasympathetic response of the hypothalamic pituitary axis (Rosas-Ballina et al., 2011). This response can activate a subset of ACh-producing T cells within the white pulp region of the spleen (Rosas-Ballina et al., 2011), an area we find to be strong in α4 and Gprin1 protein expression. By operating through a Gprin1/CDC42 signaling pathway, α4 nAChRs are implicated in T-cell proliferation and cytokine production. In the bone marrow, nicotine is found to alter stem cell number, suggestive of a role for nicotine in hematopoiesis within α4-expressing cells.

Whether the opening of the nAChR channel is necessary for the actions of nicotine in the immune system is still enigmatic. Our experiments suggest that at minimum nicotine can foster an enhanced nAChR response via the pharmacologic chaperoning of the receptor in T cells and the activation of the Gprin1/CDC42 pathway, resulting in cell proliferation and IL-6 release. Because the effects of nicotine on T-cell proliferation and cytokine release were not detected in $\alpha4^{-/-}$ mice, our findings underscore the role for the α4 subunit in the immune response but cannot dismiss the contributions of other nAChRs, including β2.

In one scenario, it is possible that IL-6 release is intimately associated with the release of additional T_H2 cytokines from T cells, shifting the immune response into T_H2 immunity

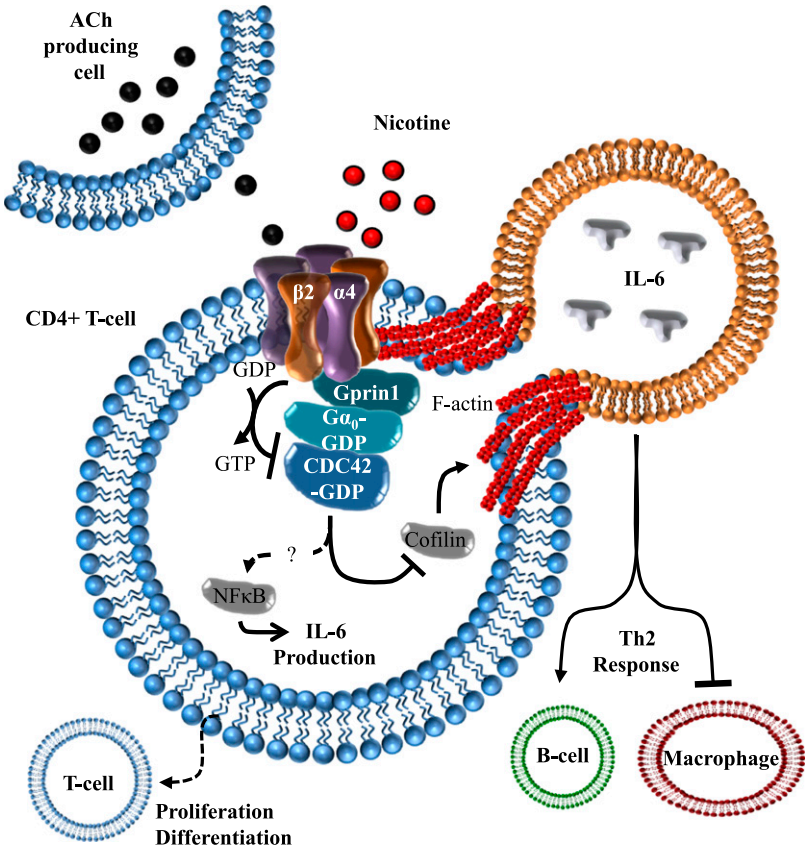

Fig. 8. Nicotine's effect on immunity via the α4 nAChR signaling pathway in T cells. Activation of α4 nAChRs by nicotine (or ACh) engages Gprin1, leading to an inhibition of $G\alpha_o$ and CDC42 (CDC42-GDP) in T cells. CDC42 regulates cytokine synthesis and release via the activation of the transcription factor NF-κB (Hobert et al., 2002) and the actin depolymerizing protein cofilin (Muller et al., 2006), respectively. This nAChR pathway may serve to regulate T-cell proliferation and T_H2 cytokine release.

(Diehl and Rincon, 2002). Studies have shown that IL-4 production promotes IL-6 release via a similar Rac/CDC42 pathway in keratinocytes (Wery-Zennaro et al., 2000), consistent with our observations on the release time course of the two cytokines in T cells. T_H2 immunologic responses are associated with adaptive immunity and increases in IgE antibody production (Ujike et al., 2002). If nicotine is indeed found to trigger T_H2 immunity in humans, our study may begin to explain the molecular connection between cigarette smoke and autoimmune disease as supported by epidemiologic evidence (Costenbader et al., 2006). For example, because both nicotine smoke and enhanced IL-6 production are shown to increase the symptoms of autoimmune diseases such as myasthenia gravis and Crohn's disease (Aricha et al., 2011; Maniaol et al., 2013), it is interesting to consider that nicotine can directly promote IL-6 production in T cells via the α4 nAChR.

Interaction with Gprin1 Mediates α4 nAChR Signaling in T Cells. Cytokines released from T lymphocytes undergo at least four regulatory checkpoints: differentiation, transcription, translation, and secretion (Cohen et al., 1974). In particular, cytokines secreted by activated $CD4^+$ T cells appear to exit the cell via remodeling of the cytoskeleton (Yoder et al., 2008). Our experiments in cultured T cells likely only address the later points. As shown in Fig. 8, our data demonstrate that nicotine, operating through an α4 nAChR/Gprin1/CDC42 pathway, can promote the formation of budding cytokine-containing vesicles via actions on the cytoskeleton, suggestive of cytokine release. This process appears dependent on the function of the α4 nAChR and the $G\alpha_o$ and Gprin1 protein complex, which can regulate the activity of CDC42. A similar $G\alpha_o$/Gprin1 mechanism of CDC42 regulation exists in neural cells and regulates neurite formation (Nakata and Kozasa, 2005). Inhibition of CDC42 in T cells is found to regulate the polymerization of actin to f-actin (Yoder et al., 2008), leading to changes in (IL-6) cytokine vesicle loading and release. This is in agreement with earlier finding that CDC42 regulates the concentration and secretion of vesicles containing a similar cytokine (IFN-γ) in T cells (Chemin et al., 2012).

In addition, CDC42 may also contribute to cytokine production via NF-κB (Hobert et al., 2002). Recent studies show that NF-κB is regulated by β2-containing nAChRs in immune cells (Hao et al., 2013). Based on our findings of an interaction between NF-κB and the α4 nAChR interactome (Fig. 1E), it is plausible that NF-κB also operates in the nicotine-driven α4 nAChR pathway underlying T-cell function.

Acknowledgments

The authors thank Drs. Thomas Loughran and Guy Cabral for comments on the manuscript, Justin King, Pierce Eggan, and Lorenzo Bozzeli for excellent technical assistance, and Drs. Yuntao Wu and Jia Guo for CEMss cells and help with the FACS analysis.

Authorship Contributions

Participated in research design: Nordman, Kabbani.
Conducted experiments: Nordman, Muldoon, Clark.
Contributed new reagents or analytic tools: Kabbani, Damaj.
Performed data analysis: Nordman.
Wrote or contributed to the writing of the manuscript: Nordman, Kabbani.

References

Amin RH, Chen HQ, Veluthakal R, Silver RB, Li J, Li G, and Kowluru A (2003) Mastoparan-induced insulin secretion from insulin-secreting βTC3 and INS-1 cells: evidence for its regulation by Rho subfamily of G proteins. *Endocrinology* **144**: 4508–4518.

Andersson J (2005) The inflammatory reflex—introduction. *J Intern Med* **257**: 122–125.

Aricha R, Mizrachi K, Fuchs S, and Souroujon MC (2011) Blocking of IL-6 suppresses experimental autoimmune myasthenia gravis. *J Autoimmun* **36**:135–141.

Barnhart MI and Lusher JM (1976) The human spleen as revealed by scanning electron microscopy. *Am J Hematol* **1**:243–264.

Chang E, Forsberg EC, Wu J, Bingyin Wang, Prohaska SS, Allsopp R, Weissman IL, and Cooke JP (2010) Cholinergic activation of hematopoietic stem cells: role in tobacco-related disease? *Vasc Med* **15**:375–385.

Changeux JP (2010) Nicotine addiction and nicotinic receptors: lessons from genetically modified mice. *Nat Rev Neurosci* **11**:389–401.

Chemin K, Bohineust A, Dogniaux S, Tourret M, Guégan S, Miro F, and Hivroz C (2012) Cytokine secretion by CD4$^+$ T cells at the immunological synapse requires Cdc42-dependent local actin remodeling but not microtubule organizing center polarity. *J Immunol* **189**:2159–2168.

Chen Z, You Y, and Zou P (2000) Methodological study of cell separation with domestic immunomagnetic beads. *J Tongji Med Univ* **20**:208–209.

Cocks BG, Chang CC, Carballido JM, Yssel H, de Vries JE, and Aversa G (1995) A novel receptor involved in T-cell activation. *Nature* **376**:260–263.

Cohen S, Bigazzi PE, and Yoshida T (1974) Commentary. Similarities of T cell function in cell-mediated immunity and antibody production. *Cell Immunol* **12**: 150–159.

Cormier A, Paas Y, Zini R, Tillement JP, Lagrue G, Changeux JP, and Grailhe R (2004) Long-term exposure to nicotine modulates the level and activity of acetylcholine receptors in white blood cells of smokers and model mice. *Mol Pharmacol* **66**:1712–1718.

Costenbader KH, Feskanich D, Mandl LA, and Karlson EW (2006) Smoking intensity, duration, and cessation, and the risk of rheumatoid arthritis in women. *Am J Med* **119**:503.e501–509.

Costenbader KH and Karlson EW (2005) Cigarette smoking and systemic lupus erythematosus: a smoking gun? *Autoimmunity* **38**:541–547.

Darsow T, Booker TK, Piña-Crespo JC, and Heinemann SF (2005) Exocytic trafficking is required for nicotine-induced up-regulation of alpha 4 beta 2 nicotinic acetylcholine receptors. *J Biol Chem* **280**:18311–18320.

Davis R, Rizwani W, Banerjee S, Kovacs M, Haura E, Coppola D, and Chellappan S (2009) Nicotine promotes tumor growth and metastasis in mouse models of lung cancer. *PLoS ONE* **4**:e7524.

Dhabhar FS, Miller AH, McEwen BS, and Spencer RL (1995) Effects of stress on immune cell distribution. Dynamics and hormonal mechanisms. *J Immunol* **154**: 5511–5527.

Diehl S and Rincón M (2002) The two faces of IL-6 on Th1/Th2 differentiation. *Mol Immunol* **39**:531–536.

García-Bernal D, Dios-Esponera A, Sotillo-Mallo E, García-Verdugo R, Arellano-Sánchez N, and Teixidó J (2011) RGS10 restricts upregulation by chemokines of T cell adhesion mediated by $\alpha4\beta1$ and $\alpha L\beta2$ integrins. *J Immunol* **187**:1264–1272.

Ge X, Qiu Y, Loh HH, and Law PY (2009) GRIN1 regulates micro-opioid receptor activities by tethering the receptor and G protein in the lipid raft. *J Biol Chem* **284**: 36521–36534.

Guo F, Hildeman D, Tripathi P, Velu CS, Grimes HL, and Zheng Y (2010) Coordination of IL-7 receptor and T-cell receptor signaling by cell-division cycle 42 in T-cell homeostasis. *Proc Natl Acad Sci USA* **107**:18505–18510.

Guslandi M (1999) Nicotine treatment for ulcerative colitis. *Br J Clin Pharmacol* **48**: 481–484.

Hao J, Shi FD, Abdelwahab M, Shi SX, Simard A, Whiteaker P, Lukas R, and Zhou Q (2013) Nicotinic receptor $\beta2$ determines NK cell-dependent metastasis in a murine model of metastatic lung cancer. *PLoS ONE* **8**:e57495.

Hawkins BT, Brown RC, and Davis TP (2002) Smoking and ischemic stroke: a role for nicotine? *Trends Pharmacol Sci* **23**:78–82.

Hobert ME, Sands KA, Mrsny RJ, and Madara JL (2002) Cdc42 and Rac1 regulate late events in *Salmonella typhimurium*-induced interleukin-8 secretion from polarized epithelial cells. *J Biol Chem* **277**:51025–51032.

Hoff J (2000) Methods of blood collection in the mouse. *Lab Anim (NY)* **29**:47–53.

Itano AA and Jenkins MK (2003) Antigen presentation to naive CD4 T cells in the lymph node. *Nat Immunol* **4**:733–739.

Kabbani N, Woll MP, Levenson R, Lindstrom JM, and Changeux JP (2007) Intracellular complexes of the $\beta2$ subunit of the nicotinic acetylcholine receptor in brain identified by proteomics. *Proc Natl Acad Sci USA* **104**:20570–20575.

Kawashima K and Fujii T (2003) The lymphocytic cholinergic system and its contribution to the regulation of immune activity. *Life Sci* **74**:675–696.

Kondo Y, Tachikawa E, Ohtake S, Kudo K, Mizuma K, Kashimoto T, Irie Y, and Taira E (2010) Inflammatory cytokines decrease the expression of nicotinic acetylcholine receptor during the cell maturation. *Mol Cell Biochem* **333**:57–64.

Küpfer S (1992) A case from practice (248). 1. Chronic idiopathic thrombocytopenic purpura with discrete splenomegaly. 2. Chronic HBV infection. Incomplete vital antigen synthesis. Minimal inflammation without signs of aggression. 3. Subacute cytomegalovirus infection (laboratory diagnosis). 4. Status following hepatitis A. 5. Nicotine abuse [article in German]. *Schweiz Rundsch Med Prax* **81**:968–970.

Lennon VA (1976) Immunology of the acetylcholine receptor. *Immunol Commun* **5**: 323–344.

Lobato-Pascual A, Saether PC, Dahle MK, Gaustad P, Dissen E, Fossum S, and Daws MR (2013) Rat macrophage C-type lectin is an activating receptor expressed by phagocytic cells. *PLoS ONE* **8**:e57406.

Maniaol AH, Boldingh M, Brunborg C, Harbo HF, and Tallaksen CM (2013) Smoking and socio-economic status may affect myasthenia gravis. *Eur J Neurol* **20**:453–460.

Marubio LM, del Mar Arroyo-Jimenez M, Cordero-Erausquin M, Léna C, Le Novère N, de Kerchove d'Exaerde A, Huchet M, Damaj MI, and Changeux JP (1999) Reduced antinociception in mice lacking neuronal nicotinic receptor subunits. *Nature* **398**:805–810.

Marubio LM, Gardier AM, Durier S, David D, Klink R, Arroyo-Jimenez MM, McIntosh JM, Rossi F, Champtiaux N, and Zoli M et al. (2003) Effects of nicotine in the dopaminergic system of mice lacking the $\alpha4$ subunit of neuronal nicotinic acetylcholine receptors. *Eur J Neurosci* **17**:1329–1337.

Middlebrook AJ, Martina C, Chang Y, Lukas RJ, and DeLuca D (2002) Effects of nicotine exposure on T cell development in fetal thymus organ culture: arrest of T cell maturation. *J Immunol* **169**:2915–2924.

Moreau T, Depierre P, Brudon F, and Confavreux C (1994) Nicotine-sensitive myasthenia gravis. *Lancet* **344**:548–549.

Müller N, Avota E, Schneider-Schaulies J, Harms H, Krohne G, and Schneider-Schaulies S (2006) Measles virus contact with T cells impedes cytoskeletal remodeling associated with spreading, polarization, and CD3 clustering. *Traffic* **7**:849–858.

Nakata H and Kozasa T (2005) Functional characterization of Gαo signaling through G protein-regulated inducer of neurite outgrowth 1. *Mol Pharmacol* **67**:695–702.

Nordman JC and Kabbani N (2012) An interaction between $\alpha7$ nicotinic receptors and a G-protein pathway complex regulates neurite growth in neural cells. *J Cell Sci* **125**:5502–5513.

Pandit TS, Sikora L, Muralidhar G, Rao SP, and Sriramarao P (2006) Sustained exposure to nicotine leads to extramedullary hematopoiesis in the spleen. *Stem Cells* **24**:2373–2381.

Quik M, Perez XA, and Bordia T (2012) Nicotine as a potential neuroprotective agent for Parkinson's disease. *Mov Disord* **27**:947–957.

Rius J, Guma M, Schachtrup C, Akassoglou K, Zinkernagel AS, Nizet V, Johnson RS, Haddad GG, and Karin M (2008) NF-κB links innate immunity to the hypoxic response through transcriptional regulation of HIF-1α. *Nature* **453**:807–811.

Rosas-Ballina M, Olofsson PS, Ochani M, Valdés-Ferrer SI, Levine YA, Reardon C, Tusche MW, Pavlov VA, Andersson U, and Chavan S et al. (2011) Acetylcholine-synthesizing T cells relay neural signals in a vagus nerve circuit. *Science* **334**: 98–101.

Ross SA, Wong JY, Clifford JJ, Kinsella A, Massalas JS, Horne MK, Scheffer IE, Kola I, Waddington JL, Berkovic SF, and Drago J (2000) Phenotypic characterization of an α_4 neuronal nicotinic acetylcholine receptor subunit knock-out mouse. *J Neurosci* **20**:6431–6441.

Russell MA, Jarvis M, Iyer R, and Feyerabend C (1980) Relation of nicotine yield of cigarettes to blood nicotine concentrations in smokers. *BMJ* **280**:972–976.

Sallette J, Pons S, Devillers-Thiery A, Soudant M, Prado de Carvalho L, Changeux JP, and Corringer PJ (2005) Nicotine upregulates its own receptors through enhanced intracellular maturation. *Neuron* **46**:595–607.

Skok MV, Grailhe R, Agenes F, and Changeux JP (2007) The role of nicotinic receptors in B-lymphocyte development and activation. *Life Sci* **80**:2334–2336.

Song DK, Im YB, Jung JS, Suh HW, Huh SO, Song JH, and Kim YH (1999) Central injection of nicotine increases hepatic and splenic interleukin 6 (IL-6) mRNA expression and plasma IL-6 levels in mice: involvement of the peripheral sympathetic nervous system. *FASEB J* **13**:1259–1267.

Sopori M (2002) Effects of cigarette smoke on the immune system. *Nat Rev Immunol* **2**:372–377.

Su IH, Dobenecker MW, Dickinson E, Oser M, Basavaraj A, Marqueron R, Viale A, Reinberg D, Wülfing C, and Tarakhovsky A (2005) Polycomb group protein ezh2 controls actin polymerization and cell signaling. *Cell* **121**:425–436.

Tracey KJ (2009) Reflex control of immunity. *Nat Rev Immunol* **9**:418–428.

Ujike A, Takeda K, Nakamura A, Ebihara S, Akiyama K, and Takai T (2002) Impaired dendritic cell maturation and increased T_H2 responses in PIR-B$^{-/-}$ mice. *Nat Immunol* **3**:542–548.

Wery-Zennaro S, Zugaza JL, Letourneur M, Bertoglio J, and Pierre J (2000) IL-4 regulation of IL-6 production involves Rac/Cdc42- and p38 MAPK-dependent pathways in keratinocytes. *Oncogene* **19**:1596–1604.

Whiting PJ and Lindstrom JM (1988) Characterization of bovine and human neuronal nicotinic acetylcholine receptors using monoclonal antibodies. *J Neurosci* **8**: 3395–3404.

Yamauchi J, Kawano T, Nagao M, Kaziro Y, and Itoh H (2000) G_i-dependent activation of c-Jun N-terminal kinase in human embryonal kidney 293 cells. *J Biol Chem* **275**:7633–7640.

Yin AH, Miraglia S, Zanjani ED, Almeida-Porada G, Ogawa M, Leary AG, Olweus J, Kearney J, and Buck DW (1997) AC133, a novel marker for human hematopoietic stem and progenitor cells. *Blood* **90**:5002–5012.

Yoder A, Yu D, Dong L, Iyer SR, Xu X, Kelly J, Liu J, Wang W, Vorster PJ, and Agulto L et al. (2008) HIV envelope-CXCR4 signaling activates cofilin to overcome cortical actin restriction in resting CD4 T cells. *Cell* **134**:782–792.

Zhang S and Petro TM (1996) The effect of nicotine on murine CD4 T cell responses. *Int J Immunopharmacol* **18**:467–478.

Address correspondence to: Nadine Kabbani, Department of Molecular Neuroscience, Krasnow Institute for Advanced Study, George Mason University, 4400 University Drive, Fairfax, VA 22030. E-mail: nkabbani@gmu.edu

The Alpha 4 Nicotinic Receptor Promotes CD4+ T-Cell Proliferation and a Th2 Immune Response

Jacob C. Nordman, Pretal Muldoon, Sarah Clark , M. Imad Damaj, Nadine Kabbani
Molecular Pharmacology

Supplementary Table 1. Expression of immune cell proteins within α4+ cells in circulation. LCI-ESI MS was used to identify marker proteins within α4+ cell derived from ICF_C. (The "+" sign indicates the cell specificity of the marker protein). A protein score (Materials and Methods) and the total number of peptides identified for each marker protein in the MS analysis is indicated.

Marker Protein	T Lymphocyte	NK	B Lymphocyte	Macrophage	Dendritic Cell	Other⌘	Protein Score	Number of Peptides
CD1d1	-	+	-	-	-	-	16.04	4
CD3	+	+	-	-	-	-	4.06	8
CD4	+++	-	-	+	+	-	8.05	9
CD5	+	+	-	-	-	-	2.05	12
CD6	+	+	-	-	-	-	4.07	8
CD8	+	+++	-	+	+	-	8.07	6
CD16	-	+	-	+++	-	+	4.04	2
CD19	-	-	+	-	-	-	10.08	8
CD28	+	-	-	-	-	-	8.06	9
CD36	-	-	-	+	-	+	8.08	3
CD44	-	-	-	-	-	+	10.04	4
CD69 p60	+	+	-	-	-	-	20.10	10
CD74	+	-	+	-	-	-	22.08	6
CD84	+	+	+	-	-	-	10.06	6
CD96	+	+	-	-	-	-	8.07	11
CD97	+	+	+	+	+	-	20.08	8
CD209	-	-	-	-	+	-	26.09	5
CD300	-	+	-	-	-	-	10.03	6
CD320	-	-	+	-	-	-	8.08	7
CCR4	+	-	-	-	-	-	10.05	12
CXCR3	+	+	-	-	-	-	10.06	9

⌘Other - Megakaryocytes, monocytes, mast cells, basophils, eosinophils, neutrophils, platelets, fibroblasts, endothelial cells, osteoblasts

The Alpha 4 Nicotinic Receptor Promotes CD4+ T-Cell Proliferation and a Th2 Immune Response

Jacob C. Nordman, Pretal Muldoon, Sarah Clark , M. Imad Damaj, Nadine Kabbani
Molecular Pharmacology

Supplementary Table 2. α4 nAChR interacting proteins from circulating ICF. Proteins isolated from an IP of the α4 nAChR using mAb299 (Fig. 1F). For each protein, a protein score (Materials and Methods), and a unique number in the NCBI database is presented.

Protein	Protein Score	Number of Peptides	NCBI
α4	16.04	16	14149758
β2	10.06	9	9506485
$G\alpha_o$	64.08	10	62643740
Gprin1	62.09	13	62663260
CDC42	6.07	4	62647125
NFκB	14.06	8	62644423

The Alpha 4 Nicotinic Receptor Promotes CD4+ T-Cell Proliferation and a Th2 Immune Response

Jacob C. Nordman, Pretal Muldoon, Sarah Clark , M. Imad Damaj, Nadine Kabbani
Molecular Pharmacology

Supplementary Table 3. Gprin1 interacting proteins from circulating ICF. Proteins coimmunoprecipitated in a Gprin1 IP (Fig. 1F). For each protein, a protein score (Materials and Methods), and a unique number in the NCBI database is presented.

Protein	Protein Score	Number of peptides	NCBI
α4	24.06	20	14149758
α9	8.07	4	12621088
β2	10.06	5	9506485
β3	10.04	4	19424304
$G\alpha_o$	16.08	16	62652225
Gprin1	14.08	33	62663260
CDC42	10.06	8	61889112
NFκB	12.06	6	62644423

The Alpha 4 Nicotinic Receptor Promotes CD4+ T-Cell Proliferation and a Th2 Immune Response

Jacob C. Nordman, Pretal Muldoon, Sarah Clark , M. Imad Damaj, Nadine Kabbani
Molecular Pharmacology

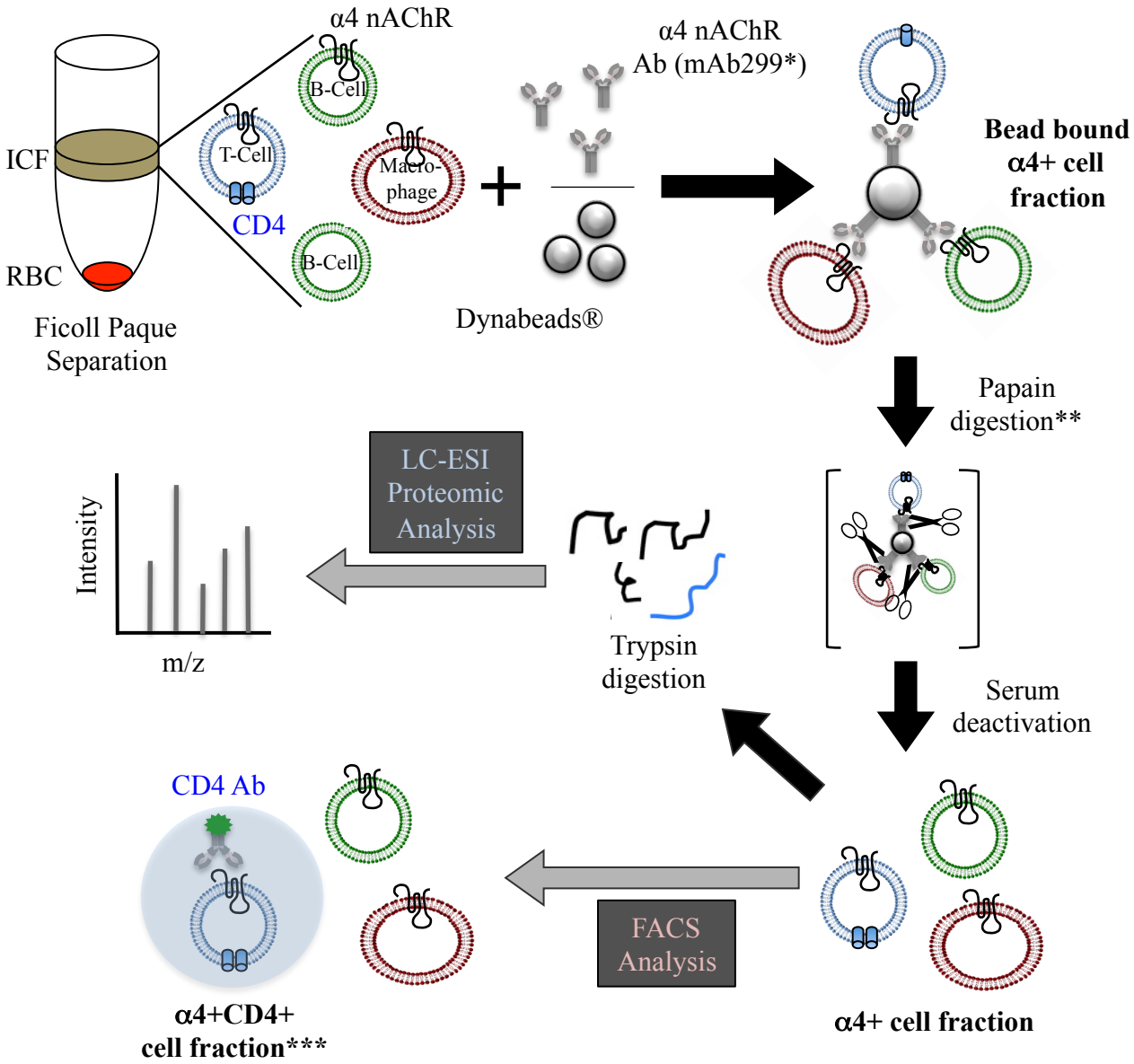

Supplementary Fig. 1. An illustration of the magnetic IgG bead cell isolation method used for LC-ESI proteomic (manuscript Fig. 1 and Supplementary Tables) and FACS analysis (manuscript Figs. 1 and 3) in the study.
*A monoclonal anti-a4 (mAb299) was optimized for cell sorting using Dynabead assay using HEK293 a4b2 cells (Sallette et al., 2005) for the isolation of a4+ cell fractions (data not shown).
** An analysis of papain digestion on the a4+ cell fraction is shown in Fig. S2.
***A monoclonal anti-a4 (mAb299) was optimized for FACS sorting of HEK293 a4b2 cells (Sallette et al., 2005) and confirmed in a4-/- in Supplementary Fig. 2.

The Alpha 4 Nicotinic Receptor Promotes CD4+ T-Cell Proliferation and a Th2 Immune Response

Jacob C. Nordman, Pretal Muldoon, Sarah Clark , M. Imad Damaj, Nadine Kabbani
Molecular Pharmacology

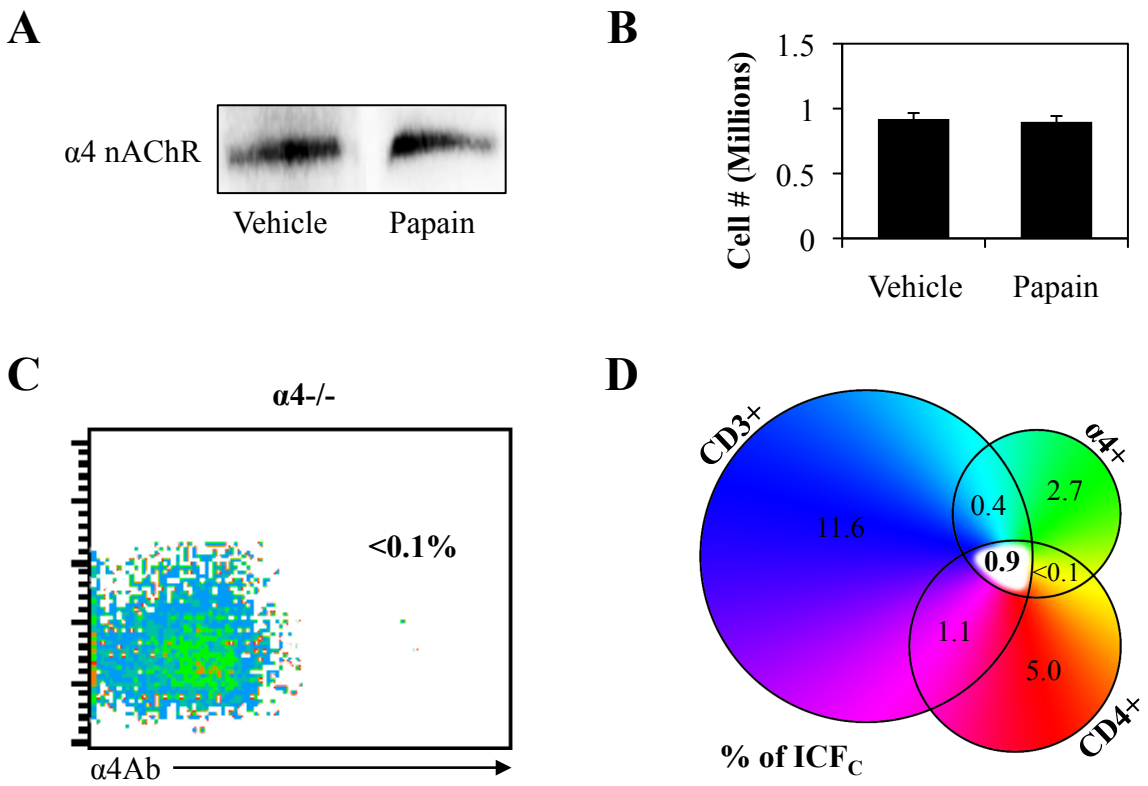

Supplementary Fig. 2. An analysis of the effect of 5 μg/ml papain on nAChR expression and cellular viability. Papain treated ICF were analyzed for (A) total α4 nAChR expression and (B) cell number. Papain treatment was found to have little to no effect on receptor expression and cell number as compared to vehicle (PBS) treatment. (C) FACS immunosorting of α4-/- cells from ICF_C using mAb299. (D) Diagram of immunocytochemical detection of α4 nAChR (green), CD4 (red), and CD3 (blue) within the ICF_C from Fig. 1D.

The Alpha 4 Nicotinic Receptor Promotes CD4+ T-Cell Proliferation and a Th2 Immune Response

Jacob C. Nordman, Pretal Muldoon, Sarah Clark , M. Imad Damaj, Nadine Kabbani
Molecular Pharmacology

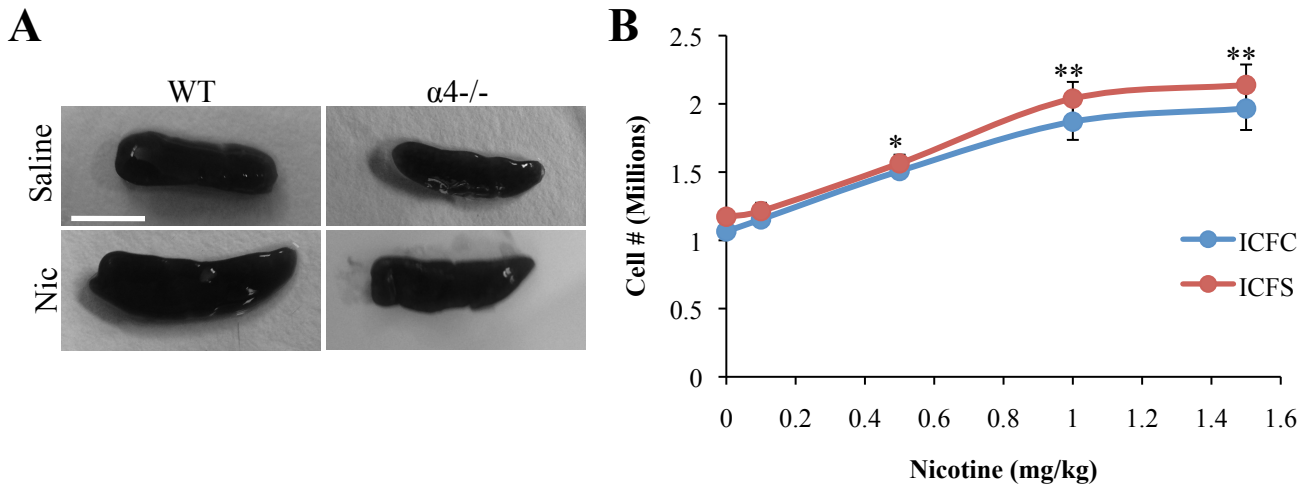

Supplementary Fig. 3. Nicotine increases spleen weight and cell number.
(A) Pictures of spleens from α4-/- and WT mice chronically injected with 1.0 mg/kg nicotine (Nic) or saline. Scale bar: 5 mm. (B) Total counted cells in ICF_C and ICF_s of nicotine treated mice.

The Alpha 4 Nicotinic Receptor Promotes CD4+ T-Cell Proliferation and a Th2 Immune Response

Jacob C. Nordman, Pretal Muldoon, Sarah Clark , M. Imad Damaj, Nadine Kabbani
Molecular Pharmacology

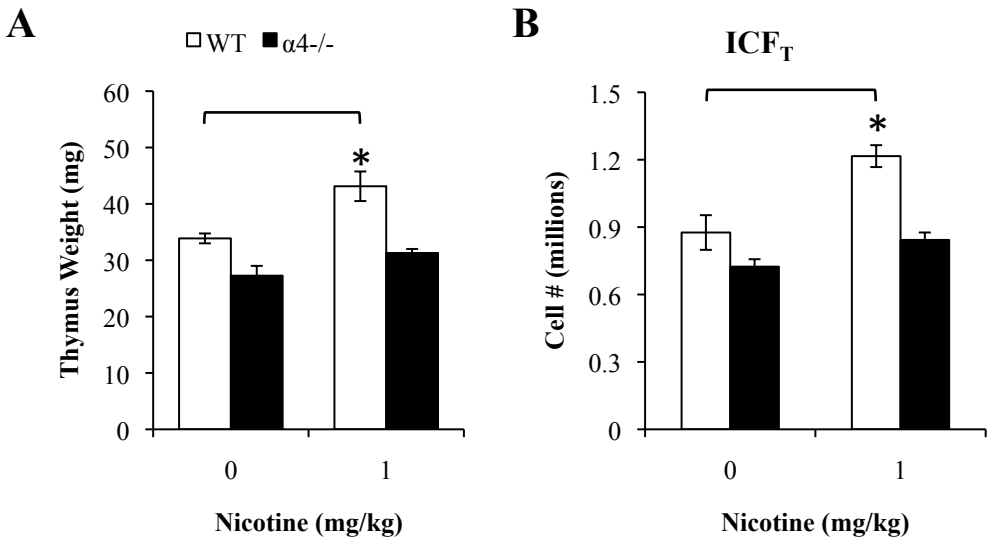

Supplementary Fig. 4. Nicotine increases thymus weight and cell number.
(A) Total weight of the thymus from α4-/- and WT mice chronically injected with nicotine (1.0 mg/kg) or saline (0). (B) Cell counts from ICF isolated from the thymus between α4-/- and WT mice chronically injected with nicotine as in *A*.

The Alpha 4 Nicotinic Receptor Promotes CD4+ T-Cell Proliferation and a Th2 Immune Response

Jacob C. Nordman, Pretal Muldoon, Sarah Clark , M. Imad Damaj, Nadine Kabbani
Molecular Pharmacology

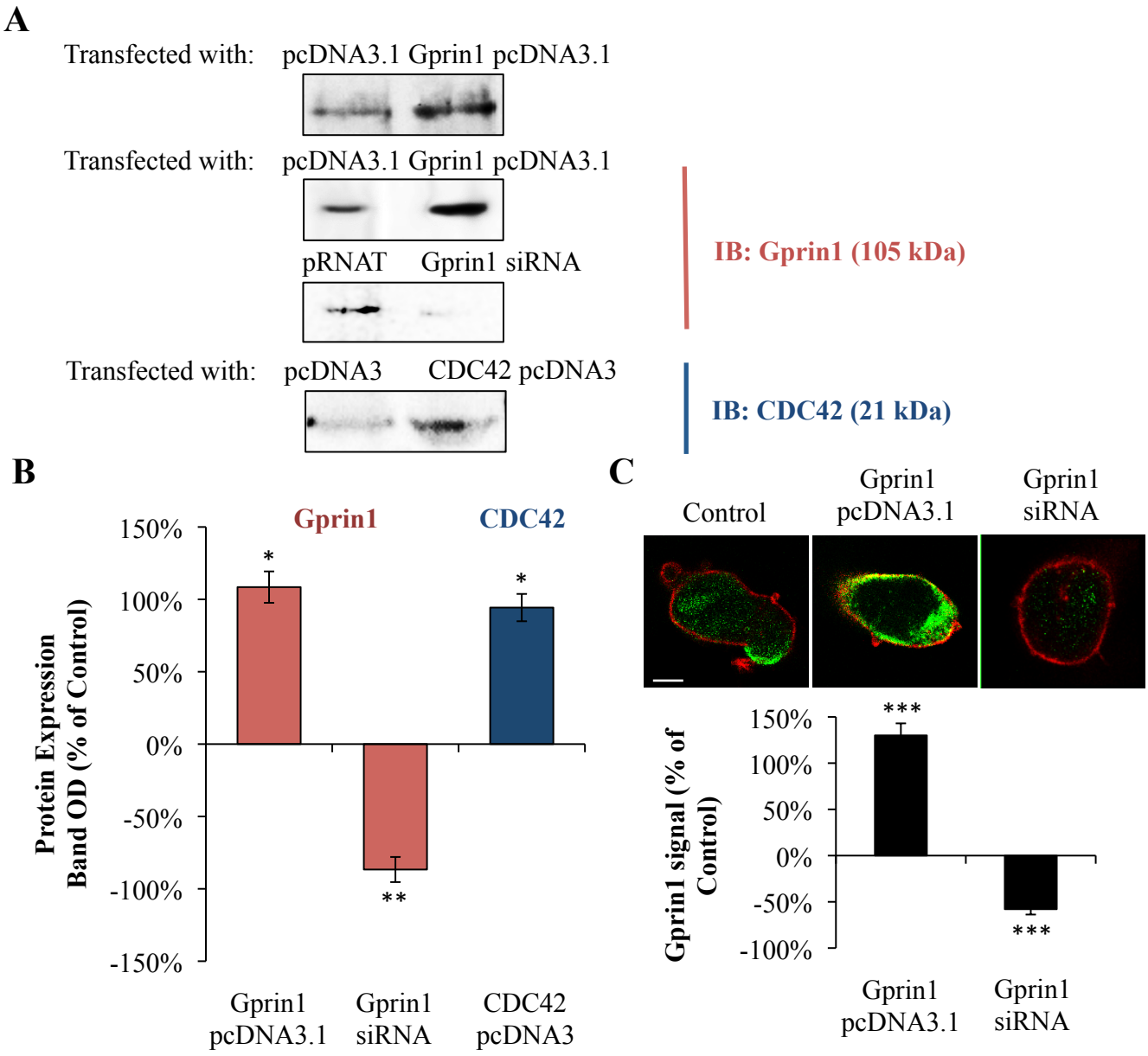

Supplementary Fig. 5. Genetic regulation of Gprin1 and CDC42 expression in cells. (A) Western blot detection of endogenous Gprin1 and CDC42 in CEMss cells. Cells were transiently transfected with the indicated plasmids as described in (Materials and Methods). An empty vector was used as a control. (B) Band density analysis of the blots quantifying change in the level of Gprin1 and CDC42 following transfection. (C) ICC confirmation of Gprin1 expression vectors in CEMss. Cells were probed with rhodamine phalloidin (red) and Gprin1 Abs (green). Adjoining histogram is of fluorescence analysis of Gprin1 signal in Gprin1 pcDNA3.1/siRNA transfected cells as a percent of control. Scale bar: 1 μm.